GENERAL ELECTRIC

Research Laboratory

ROUGHNESS, BLUNTNESS, AND ANGLE OF ATTACK EFFECTS ON HYPERSONIC BOUNDARY LAYER TRANSITION

by

H.T. Nagamatsu, B.C. Graber, and R.E. Sheer, Jr.

Report No. 64-RL-(3829 C) November 1964

55-P 8.0

GENERAL ELECTRIC

Research Laboratory

REPORT NO. 64-RL-(3829 C)

ROUGHNESS, BLUNTNESS, AND ANGLE OF ATTACK EFFECTS ON HYPERSONIC BOUNDARY LAYER TRANSITION

H. T. Nagamatsu, B. C. Graber, and R. E. Sheer, Jr.

November 1964

Published by
Research Information Section
The Knolls
Schenectady, New York

ABSTRACT

An investigation was conducted in a hypersonic shock tunnel to study the laminar boundary layer transition on a highly cooled 10° cone of 4-foot length over the Mach number range of 8.5 to 10.5 with a stagnation temperature of 1400°K. The effects on transition of tip surface roughness, tip bluntness, and ±2° angle of attack were investigated. With fast response thin film surface heat transfer gauges, it was possible to detect the passage of turbulent bursts that appeared at the beginning of transition. Boundary layer pitot tube surveys and schlieren photographs were obtained to verify the interpretation of the heat transfer data. It was found that the surface roughness greatly promoted transition in the proper Reynolds number range. The Reynolds number for the beginning and end of transition at the 8.5 Mach number location were 3.8×10^6 to 9.6×10^6 and 2.2×10^6 to 4.2×10^6 for the smooth sharp tip and rough sharp tip, respectively. The local skin friction data, determined from the pitot tube survey, agreed very well with the heat transfer data through Reynolds analogy. The tip bluntness data showed a strong delay in the beginning of transition for a cone base to tip diameter ratio of 20, approximately a 35% increase in Reynolds number over that of the smooth sharp tip case. The angle of attack data indicated the cross flow to have a strong influence on transition by promoting it on the sheltered side of the cone and delaying it on the windward side.

Manuscript received October 20, 1964.

Nomenclature

C_f	local skin friction coefficient
C_R	local heat transfer coefficient
C_P	specific heat at constant pressure
H_o	free stream stagnation enthalpy
H_w	model wall enthalpy
I_o	constant current through heat gage, amps
k	thermal conductivity
M	Mach number
P	pressure
P'_o	free stream pitot pressure
P'_{o_4}	boundary layer pitot pressure
q	local heat transfer rate, BTU/ft^2-sec.
Re_x	Reynolds number based on cone surface distance
Re_θ	Reynolds number based on momentum thickness
ΔRe_{tr}	incremental change in the beginning transition Reynolds number
R_o	initial heat gage resistance prior to run
T	temperature
u	local velocity
y	distance measured perpendicular to model wall
α	angle of attack
α_2	heat gage resistance variation coefficient
δ	local boundary layer thickness
ϱ	local density
σ	Prandtl number

Subscripts

b	backing material for heat gage
i	incompressible flow conditions
1	local conditions outside boundary layer
5	nozzle reservoir conditions

ROUGHNESS, BLUNTNESS, AND ANGLE OF ATTACK EFFECTS ON HYPERSONIC BOUNDARY LAYER TRANSITION*

H. T. Nagamatsu, B. C. Graber, and R. E. Sheer, Jr.
Mechanical Investigations Section
CHEMISTRY RESEARCH DEPARTMENT

I. INTRODUCTION

There is a need for knowledge regarding the laminar boundary layer transition at high Mach numbers for the development of advanced nose cones, satellites, and space vehicles. Above a Mach number of 8, there is no theoretical and only limited experimental information available. The re-entry nose cone design engineers are thus faced with extrapolating the lower Mach number data to the re-entry velocities. In doing this, a conservative design will usually result since it will be necessary to use protection against turbulent boundary layer heating. With transition data in the high Mach number range, it would then be possible to more accurately predict the necessary heat protection.

* This research was partially supported by the Ballistics System Division, United States Air Force.

Another application for the boundary layer transition knowledge would be in the design of a space plane which will be operating in the Mach number range of 5 to 26. The engine inlet ramps for this type of plane would most likely be very long which would favor boundary layer transition which in turn would produce increased boundary layer growth, higher heat transfer rates, and varying inlet performance. Therefore, theoretical and experimental information on boundary layer phenomena at high Mach numbers is imperative as more sophisticated concepts are developed for future space vehicles.

The stability of the laminar boundary layer flows to small disturbances has been investigated by a number of authors[1-5] for both incompressible and compressible flows. The theoretical analysis show good agreement with the experimental results up to Mach numbers of about 3, but disagree at the higher Mach numbers. For example, the recent theoretical work of Lees and Reshotko[5] predicts the experimental data of Laufer and Verbalovich[6] at Mach numbers of 1.6 and 2.2 very well; but the theory does not agree with the results of Demetriades[7] at a Mach number of 5.8, where it is an order of magnitude lower in Reynolds number than the experimental data. Therefore, an improved stability theory which would be applicable to Mach numbers greater than 3 is necessary.

The mechanism for the actual breakdown of the laminar boundary layer is still not completely understood. For incompressible flow, the existence of Tollmien-Schlichting waves, which agree with theory, has been confirmed experi-

mentally by Schubauer and Skramstad.[8] Schubauer and Klebanoff[9] indicated that the transition consisted of the formation of turbulent spots which grow into completely turbulent flow. The recent work of Klebanoff, Tidstrom, and Sargent[10] indicated that the three-dimensional perturbations dominated the turbulent spot or burst formation. Thus the transition for an incompressible flow starts with the formation of turbulent bursts.

For supersonic and hypersonic flows up to a Mach number of 8, Laufer and Verbalovich[6], Demetriades[7], and Potter and Whitfield[11] have shown the existence of Tollmien-Schlichting waves in the laminar boundary layer. Potter and Whitfield used hot-wire anemometers to follow the disturbances in the boundary layer but were unable to detect any particular turbulent burst action. All three sets of data were obtained in continuous flow facilities, and as a result, the facility itself could possibly mask the turbulent bursts on the model. If there was turbulent flow on the nozzle wall, this probably introduced enough disturbance into the main flow to obscure the turbulent burst action on the model in what would appear to be background noise of the instrumentation.

In the firing range, there is negligible disturbances ahead of the model with the result that turbulent bursts have been observed on slender models at supersonic speeds. Jedlicka, Wilkins, and Seiff[12] fired slender ogive-cylinder models at a Mach number of 3.5 and observed the turbulent bursts followed by a laminar boundary layer similar to what had been noticed by Schubauer and Klebanoff at subsonic velocities with hot-wire probes. Lyons and Sheetz[13] and Levensteins[14] fired

10° cone models in the Naval Ordnance Laboratory Pressurized Ballistic Range at Mach numbers of 3.1 and 3.8 and also noticed the turbulent bursts at the beginning of transition. In both of these cases, the schlieren and shadowgraphs showed the turbulent bursts to be accompanied by weak shock waves emanating out into the flow about the body. The conclusion is thus reached, based on the available literature, that transition begins with the appearance of turbulent bursts. Further evidence will be given for this conclusion by the data presented in this report.

Aside from the basic mechanism of transition, there is still the question of the effects of Mach number, surface roughness, bluntness, angle of attack, real gas, etc., on the laminar boundary layer transition. This report will attempt to contribute some insight to the surface roughness, bluntness, and angle of attack effects for Mach numbers greater than 8. Sputtered platinum surface heat transfer gages were used in place of the hot-wire anemometer to monitor the laminar boundary layer stability. The response of these gages is approximately one microsecond as compared to about 10 microseconds for the hot-wire. The heat gages indicated the passage of the turbulent bursts and established their speed by measuring the transit time over successive gages along the cone surface.[15] It was determined that the burst moved at 0.9 of the free-stream velocity which makes the disturbance subsonic. A pitot tube survey[16] of the boundary layer was made at various reservoir conditions to verify the existence of the different types of boundary layers: laminar, transition, and turbulent. Schlieren

photographs of the boundary layer were also obtained and gave support to the other data. With the various techniques, it was always possible to detect the occurrence of transition.

This report is one in a series of reports on a continuing study of laminar boundary layer transition on a 10° cone at hypersonic Mach numbers. More detailed information can therefore be found in Refs. 15 and 16 on the earlier heat transfer, schlieren, and pitot tube boundary layer survey results.

II. EXPERIMENTAL EQUIPMENT AND INSTRUMENTATION

A. Hypersonic Shock Tunnel

All of the tests were conducted in a hypersonic shock tunnel with a 24 in. diameter conical nozzle attached to a 103-foot long constant area driven tube. A detailed description of the tunnel and the associated instrumentation is presented in Ref. 17. Combustion of a stoichiometric mixture of hydrogen and oxygen with an excess of helium was used in the driver to produce the desired shock wave in the driven tube. The shock wave reflects from the nozzle entrance and further increases the pressure and temperature. An aluminum diaphragm at the nozzle entrance permits the evacuation of the dump tank and nozzle to a few microns of mercury to facilitate the flow establishment and minimize the strength of the starting shock waves.

B. Model

The cone model of 4-feet in length with a 10° included angle was made in five pieces with five pressure orifices and six heat gages.[15] To simplify the investigations of the leading edge roughness and bluntness, the tips shown in Fig. 1 were made interchangeable. In this report, the various tips will be referred to as designated in Fig. 1. For the sharp tips, the leading edge diameter was approximately 0.002 inches. The first static pressure measuring location on the model was 2.709 in. from the tip and was constructed with a series of 0.032 diameter holes around the circumference connected to a cavity holding the pressure transducer. Other 0.125 in. diameter static pressure orifices were located at 13.728, 24.730, 35.520, and 46.541 in. from the cone tip with the 35.520 location being used for the boundary layer survey.[16] The heat gages were located on the opposite side of the cone, 180° from the pressure gages, at 18.722, 22.757, 26.742, 35.396, 40.377, and 45.380 in. from the cone tip. The surface of the cone had approximately a 50 micro-inch finish. The model was mounted on a 6 in. hollow sting which was independently supported and vibrationally isolated from the dump tank through Teflon bushings.

C. Instrumentation

Lead-zirconate-titinate piezoelectric pressure gages, described in Ref. 15 were used to measure the static pressure on the cone surface and the pitot tube pressure throughout the boundary layer. The pressure gages were dynamically calibrated in an 8-inch calibration shock tube over the pressure range encountered in the test section.

For measuring higher pressures such as the free stream impact and reflected shock wave pressures at the entrance to the nozzle, the standard Kistler SLM quartz pressure transducers were used. The output of these gages is much lower than that for lead-zirconate-titinate but are less sensitive to vibrations and temperature. Thus, they are ideal for measuring high pressures in the shock tunnel. The Kistler gage used in the free stream impact probe was dynamically calibrated in the 8-inch tube and the reflected pressure gages were calibrated with a dead weight tester.

A single pass Schlieren system with 6-foot focal length parabolic mirrors was used to obtain the photographic records of the shock waves and the viscous layers. To obtain good resolution, a spark of about 0.4 microsecond duration was used as the light source.[17]

The surface heat transfer gages were made of platinum sputtered on a pyrex backing to a thickness of approximately 350 Å. To prevent shorting out the platinum film during high temperature tests, a thin evaporated film of silicone dioxide was placed over the platinum to electrically insulate it. This coating did not appreciably affect the gage response time which remained about one to two microseconds. The heat gages were all dynamically calibrated in the 8-inch calibration shock tube with the gage characteristics being determined as described in Ref. 18.

III. EXPERIMENTAL PROCEDURES AND RESULTS

The conditions in the test section of the shock tunnel are essentially determined by the nozzle area ratio and the conditions behind the reflected shock at the entrance to the nozzle.[17,19,20] The equilibrium stagnation temperature and pressure behind the reflected shock wave are controlled by the strength of the incident shock wave and the initial temperature and pressure in the driven tube. With a combustion driver it is possible to operate over a wide range of reflected temperatures and pressures.

The pressure, P_5, behind the reflected shock wave was measured with a standard Kistler quartz gage and the corresponding reflected stagnation temperature, T_5, was calculated using the known shock velocity at the end of the driven tube and the equilibrium thermodynamic data for air.[21-23] To obtain information regarding the air expansion process in a hypersonic nozzle, an investigation of the static and impact pressures along the axis of the nozzle was conducted and detailed results are presented in Refs. 17, 19, and 20. For the present investigation, the reservoir conditions were chosen such that T_5 = 1400°K while P_5 varied from 450 psia to 2200 psia. These reservoir pressures were high enough to have nearly equilibrium conditions before and after the air was expanded in the nozzle. The reservoir pressure variation essentially represented a Reynolds number variation at any given model location.

The test section conditions were determined by using a 3/4 in. hemisphere tip impact probe. A typical time history of the output of this probe divided by the reflected pressure, P_5, is shown in Fig. 2. As indicated the reflected reservoir

pressure decreases with time while the P_o'/P_5 ratio remains almost constant over a two millisecond period. When this ratio is converted to Mach number, it is observed that the test section Mach number is nearly constant over the corresponding period which indicates that the real gas effects are small as stated before. The flow establishment time for the shock tunnel was about 0.7 milliseconds which explains why Fig. 2 neglects the first millisecond. Therefore, the effective test time of the facility was two milliseconds which was sufficient for the present investigation.

Since a conical nozzle giving source type flow was used in the study, the cone model was mounted such that 29 inches of it extended up into the nozzle. In this configuration it was necessary to check the inviscid flow over the model. As indicated in Fig. 3, the cone surface pressure shows a smooth variation with simply a uniform increase over the empty nozzle case. This indicates that there is no large disturbances to the flow inside the nozzle, and it also demonstrates that the flow outside the nozzle was expanding as a free-jet. This free-jet expansion was most likely due to the low back pressure since the dump tank was evacuated to 3 microns of mercury prior to any shot. The low dump tank pressure also reduced the starting shock strength which in turn decreased the instrumentation noise.

With the present nozzle model configuration and source type flow, a Mach number and pressure gradient existed along the cone surface. The Mach number varied from 8.5 to 10.5 over the six surface heat transfer gages. For hypersonic flow expansion, the local temperature, hence speed of sound, decreases so as to counteract the increasing Mach

number gradient thus having the local velocity remain almost constant. This type of variation is not true for subsonic flow where a Mach number increase means a velocity increase. For the present tests, the velocity varied from 5630 to 5744 ft/sec over the 6 heat gages which gave a 4.29 ft/sec/in increase. Weil[24] has calculated the effects of velocity and pressure gradients for compressible flow, based upon the theory of Lin and Lees,[4] and found that they are negligible for a free-stream Mach number of 4. As is known, free stream gradients do affect the stability of incompressible and low supersonic boundary layer flows. Without a reliable hypersonic stability theory, it is impossible to predict whether or not these gradients are important at hypersonic Mach numbers. Nevertheless with the previously stated free stream gradients present, laminar, transition, and fully turbulent flow were obtained and will be discussed in the next section.

The boundary layer surveys presented were conducted with a circular pitot tube probe placed in the number four static pressure orifice. A picture of the configuration can be found in Ref. 16. The inside diameter of the tube was 0.090 inches with a 0.005 inch wall thus allowing for reasonable response time and limited detrimental probe effects. As to the probe response, Fig. 2 shows the typical laminar and turbulent P'_{o_4}/P_5 ratios. After the initial increase, the ratio was constant indicating steady flow. This was not the picture for the transition flow as will be pointed out later where the pitot tube showed large oscillations.

The angle of attack data was obtained by pitching the cone model to plus and minus two degrees. The cone surface pressure and heat transfer gages were kept in the vertical plane with respect to the pitch axis. Also, the two degree pitch was performed such that the cone tip remained on the nozzle axis. Again, the question presented itself as to the effect of this configuration on the basic nozzle flow. As was the case with the zero angle of attack, the measured cone surface pressure variation remained smooth and changed only in magnitude as the angle of attack changed from plus to minus. Thus, the indication was that this configuration did not disturb the basic flow to any greater extent than the zero angle of attack configuration.

IV. DISCUSSION OF RESULTS

A. Effects of Surface Roughness

1. Heat transfer

The output from the heat gages was converted to local heat transfer rates by using the equation

$$q(t) = \frac{\sqrt{\pi}}{2} \frac{\sqrt{(\rho C_p k)_b}}{\alpha_2 I_o R_o} \left\{ \frac{\Delta E(t)}{\sqrt{t}} + \frac{1}{\pi} \int_0^t \frac{\sqrt{\frac{\lambda}{t}}\Delta E(t) - \Delta E(\lambda)\, d\lambda}{(t-\lambda)^{3/2}} \right\} \tag{1}$$

where $\sqrt{(\rho C_p k)_b}/\alpha_2$ is the gage characteristic determined in the calibration tube. This equation was integrated on the G.E. 225 computer which greatly simplified the data reduction. The local heat transfer rates were converted to heat transfer

coefficients by using the expression

$$C_h = \frac{q}{\rho_1 u_1 (H_o - H_w)} \tag{2}$$

Initially, the discussion of the heat transfer data presented in Figs. 4 to 11 will be limited to the effects of roughness on the sharp tip cone configuration. The laminar and turbulent theories presented in these figures were calculated from the work of A. D. Young[25] and Persh[26] respectively using the Reynolds analogy of

$$C_h = \frac{C_f}{2\sigma^{2/3}} \tag{3}$$

where σ is the Prandtl number taken as 0.72 for air. Since both of these theories were flat plate theories, the transverse curvature correction of $\sqrt{3}$ was used in the laminar case. For the turbulent case, no transverse curvature correction was used on the flat plate theory, and as will be shown, good agreement with the present cone data was obtained.

As indicated earlier, there exists an increasing Mach number gradient, 8.5 to 10.5 over the six heat gages, and a decreasing pressure gradient along the cone surface. This tends to complicate the discussion of the local surface heat transfer distribution along the cone surface, and as a result, only one gage location will be discussed so as to limit the variables and simplify the explanation of the various reservoir pressures. The first heat gage, located 18.722 in. from the cone tip will be used as the representative gage for the discussion of the smooth and rough sharp tip

configurations with the model at zero angle of attack. The Mach number at this gage location is 8.5. It should be understood that any one of the six heat gage locations could be used to follow transition as Reynolds number, based on distance along the cone surface, is increased. The discussion would be exactly the same for each gage location.

Throughout the present study, the reservoir temperature, T_5, was held at approximately 1400°K while the reservoir pressure, P_5, was varied which in turn varied the Reynolds number at the first heat gage location. The lowest reservoir pressure investigated was $P_5 = 450$ psia, shown in Fig. 4. Both the smooth and rough sharp tip configuration gave a smooth heat transfer trace with all the data scatter being contained within the symbols. The magnitude of both configurations was about the same and was displaced about 30 percent above the laminar theory. The Reynolds number for this reservoir condition was 1.95×10^6 at the first heat gage. Since the heat gage traces were smooth with no noticeable oscillations, uniform laminar flow was undoubtedly present for both the smooth and rough tips. Tip roughness therefore had no effect on the laminar boundary layer when the Reynolds number was low enough. The agreement of the data with the laminar theory is poor, but this could be due to the fact that the pressure gradient is not accounted for in the flat plate theory.[25] About 30 percent deviation in the heat transfer magnitude between theory and experiment was observed for all laminar cone flow. The existence of the laminar flow was verified by a boundary layer survey as discussed in the next section.

At the next higher reservoir pressure of P_5= 585 psia, Fig. 5, the Reynolds number at the first heat gage was 2.55×10^6. Again, the smooth sharp tip gave a smooth, uniform trace indicating laminar flow. It was found after extensive examination that at this reservoir pressure and Reynolds number the first heat gage for the rough tip configuration was in the very beginning of transition where some turbulent bursts started appearing over the gage. Thus, the rough sharp tip as compared to the smooth tip introduced enough disturbances, which were amplified, to cause the formation of turbulent bursts. Increasing the reservoir pressure to 760 psia placed the rough tip well into the transition region, Fig. 6. The Reynolds number was 3.3×10^6, and at this condition the heat transfer magnitude with large fluctuations approached the emperical turbulent theory. The transition occurred with the appearance of the turbulent bursts which showed up on the fast response heat gage as a pulse oscillation followed by a smooth trace indicating the return to laminar flow after the passage of the turbulent burst as observed by others at lower speeds, Refs. 10, 12, 13.

The next higher reservoir condition, P_5=890 psia, increased the Reynolds number to 4×10^6 at the first heat gage, Fig. 7. For this condition, the heat transfer magnitude for the rough sharp tip compares quite well with the turbulent theory, and the heat gage trace for the rough tip indicated no large oscillations as in the transition case but only small high frequency oscillations which are characteristic of the fully turbulent boundary layer.

On the other hand, the smooth tip shows large oscillations in the heat transfer value with the magnitude less than the rough tip value and turbulent theory which indicates the smooth tip boundary layer to be in the transition flow. Thus, the rough sharp tip has disturbed the boundary layer enough to force nearly fully turbulent flow at the first heat transfer gage while the smooth tip has only reached transition flow for a Reynolds number of 4×10^6.

From the heat gage traces showing transition flow, it was possible to determine the velocity of any turbulent burst as it moved over successive heat gages along the cone surface. This information showed that the burst is moving at approximately 0.9 of the gas velocity outside the boundary layer.[15] This places the point of maximum oscillation near the outer edge of the boundary layer. Using a hot-wire technique, Potter and Whitfield[11] found the critical height, defined as the location of maximum hot-wire output, to be approximately 0.92 of the boundary layer thickness for a Mach number of 8 and an insulated wall condition. At subsonic speeds, the critical height is approximately 0.22 of the boundary layer thickness as observed experimentally by Klebanoff, Tidstrom, and Sargent.[10] The present critical height for the cool wall case seems to agree with Potter and Whitfield's insulated wall results. Therefore, the large critical height location might explain why cooling was not entirely effective in stabilizing the laminar boundary layer at hypersonic Mach numbers since transition was obtained in the present work with a wall to stagnation temperature ratio of 0.214.

Increasing the reservoir pressure as shown in Figs. 8 to 11, the rough sharp tip remained in fully turbulent flow while the smooth sharp tip stayed in transition flow until P_5 = 2200 psia. The respective Reynolds numbers at these conditions were 5.7 x10^6 at P_5 = 1300 psia, 7.3 x10^6 at 1800 psia, and 9.6 x10^6 at 2200 psia. Hence, the natural transition on the smooth tip cone required a Reynolds number of 9.6 x10^6 to become fully turbulent while the rough tip forced transition and allowed fully turbulent flow to form at a Reynolds number of 4 x10^6. Tip roughness as used in this study was thus very effective in promoting boundary layer transition. It might also be noted that once fully turbulent flow was developed, the local heat transfer rates agreed quite well with the turbulent theory for both the smooth and rough tip configurations. Also, the local heat transfer oscillations for the smooth and rough tip turbulent flows were small compared to the transition flow.

The local heat transfer rates were reduced to coefficient form as previously indicated. When the heat transfer coefficients were plotted against Reynolds number, based on cone surface distance, the results shown in Fig. 12 were obtained. This graph deals only with the first heat gage which was located 18.722 in. from the cone tip where the local Mach number outside the boundary layer was 8.5. Fig. 12 essentially presents in summary form the information discussed in the previous series of figures. The graph shows the initial flow at low Reynolds number to be laminar with no oscillations. As the Reynolds number increases, the boundary layer flow moves into the transition region with large

oscillations due to the passage of turbulent bursts over the gage. When fully turbulent flow is reached for either the rough or smooth tip, the oscillations become high in frequency and small in magnitude. The difference between the smooth and rough surfaces upon the transition of the boundary layer is very evident from this figure. The roughness greatly reduces the length of the transition region as compared to the smooth case. Once a high enough Reynolds number is reached, roughness forces the boundary layer over to turbulent flow very rapidly.

2. Schlieren Photographs

Schlieren photographs were obtained to support the previous interpretation of the heat transfer data. A composite series of pictures with the smooth tip on the top and the rough tip model on the bottom are presented in Fig. 13. To obtain this series of photographs, it was necessary to advance the cone further into the nozzle for each successive picture since the schlieren windows on the dump tank were at a fixed location just downstream of the nozzle exit. Fig. 13 demonstrates visually that boundary layer transition was actually obtained. For the smooth tip cone, all the photographs from left to right show a well defined light to dark boundary which locates the outer edge of the hypersonic laminar boundary layer. A hypersonic laminar boundary layer can be seen with a schlieren system since a steep density gradient exists at the outer edge of the layer. It should be noted that the two right-hand photographs for the smooth tip show some eddies in the light to dark boundary which suggests the presence of turbulent bursts. For comparison

purposes, the heat traces for these conditions are presented under the corresponding photographs. All the heat traces are smooth following nozzle flow establishment except for the last two right-hand traces which show small oscillations in the first and large burst type oscillations in the second. The first set of traces indicate the very beginning of transition while the second demonstrates that transition is further along.

The rough tip configuration, lower series of photographs in Fig. 13, indicate the existence of laminar boundary layer flow in the first three photographs to the left. The corresponding heat traces are also smooth indicating laminar flow. The next three photographs to the right show the light to dark boundary fading out into a waffle type effect due to the turbulent eddy motion. This is thus indicative of the turbulent flow since the turbulent eddy action would tend to eliminate the sharp density gradients. The corresponding heat gage traces for the two right hand photographs of the rough tip cone show very small high frequency oscillations. Hence the schlieren composite photographs verify the local heat transfer interpretation and gives further evidence of the existence of laminar boundary layer transition.

3. Boundary Layer Survey

A further check on the existence of the various boundary layers was made by probing the layer with a pitot tube. The initial portion of this work was conducted and reported in Ref. 16. So far, the discussion has centered on the 8.5 Mach number location along the cone. In order to have a

sufficiently thick boundary layer, for probing, it was necessary to move back to the Mach number 10 location, fourth pressure gage. This will not change the basic discussion and results because once a given location along the cone surface becomes fully turbulent, all positions downstream of it are turbulent. Also as stated earlier, our previous transition discussion would hold true regardless of which heat gage had been initially selected.

The boundary layer probing was extended far enough from the wall to measure not only the pitot pressure within the boundary layer but also the pressure just outside. The results of this investigation are presented in non-dimensional form in Fig. 14 where the pitot pressure within the boundary layer is divided by that in the free stream. The laminar and turbulent profiles show very little oscillation while the transition one indicates large oscillations. It is interesting to note that the pitot response time was fast enough to follow some of the turbulent burst oscillations in the transition region. Also, it is observed that the major oscillations occur towards the outer edge of the boundary layer which agree with the heat transfer data in that the turbulent bursts are moving at 0.9 of the free-stream velocity. The different profiles were obtained at a reservoir temperature of 1400°K and the following reservoir pressures: smooth tip laminar P_5 = 585 psia (Fig. 15), rough tip turbulent P_5 = 1300 psia, and smooth tip turbulent P_5 = 2200 psia. In Fig. 14 the smooth and rough sharp tip turbulent profiles are exactly the same. Hence, it makes little difference at hypersonic Mach numbers how a boundary layer becomes turbulent because once it is established,

it has no past history of any disturbance effects. This same result can be seen in Figs. 16 to 18, for the other profiles of velocity, density, and temperature.

In order to reduce the boundary layer impact pressure data to obtain velocity, temperature, density, and Mach number profiles, it was necessary to make several assumptions because it was not possible to measure the temperature variation through the boundary layer. The assumptions used were as follows: (1) Ideal gas flow exists in the test section, $\gamma = 1.4$; (2) Constant wall temperature with $T_w = 300°K$; (3) Static pressure constant across the boundary layer; (4) Prandtl number equal to unity; (5) Total energy constant across the boundary layer.

The first assumption is quite satisfactory since at the reservoir temperature of 1400°K and for the stagnation pressures employed, the real gas effects were very small with the flow expanding in equilibrium.[19,20] A short test period of approximately 2.0 milliseconds justifies the second assumption in that there is not enough run time involved for the surface temperature to change significantly. The constant static pressure assumption is a standard one for boundary layer analysis. The last two assumptions are the important ones and have strong implications with respect to the profiles obtained. By assuming a Prandtl number of unity and constant total energy across the boundary layer, one is thus supposedly dealing with the insulated wall case of no heat transfer. This is not the situation for the present experimental investigation, and as a result, the calculated profiles obtained should be taken as only a first approximation to the true profiles. The actual test situation is one of a cool wall

with heat transfer where $T_w/T_o = 0.214$. Nevertheless, the above assumptions should hold fairly well in the outer portion of the boundary layer where the temperature is close to that of the free stream. The validity of these assumptions decreases as one approaches the wall where the heat transfer effect becomes important.

By comparing the velocity profiles for the three types of flows, Fig. 17, it is noted that there is a large difference between the laminar, transition, and turbulent cases. The assumptions used in calculating the profiles make them approximate next to the wall, but by considering the impact-pressure variations as presented in Fig. 14, it is observed that there is a significant difference at $y = \delta/2$. Using this as a guide, it can be concluded that the difference in the flows existed and was not due entirely to the assumption employed in the calculations. Also, the assumption of constant enthalpy should be reasonably good for the outer half of the boundary layer regardless of the wall heat transfer rates. By comparing the present results with other data available in the literature[27] where total temperature through the boundary layer was measured as well as impact pressure, it was estimated from this data that a maximum error of 50 percent could exist in the present calculated temperature next to the wall. This 50 percent error would result in a 25 percent maximum error in the calculated velocity. This error would not account entirely for the observed differences in the profiles, and it would not change the conclusion that laminar, transition, and turbulent flow actually existed at 34.52 inches from the cone tip for the various test conditions. The boundary layer survey thus gave further support to the inter-

pretation of surface roughness effects, and it also demonstrated that the induced turbulent flow is the same as natural turbulent flow.

From the velocity profiles the local skin friction coefficients were determined. When the local skin friction coefficient was converted to a corresponding heat transfer coefficient, through the Reynolds analogy, it was found that very good agreement existed between the boundary layer profile data and the local heat transfer data. This agreement helped to verify that the above assumptions, used in determining the various profiles from the pitot tube data, had very limited effects on the final profile shapes.

For the present turbulent data, the skin friction coefficient was divided by the incompressible one and presented in Fig. 19. A compairson is made to other experimental data[27-30] and theories[31-33] in this figure. It can be seen that the present data agrees reasonably well with the other data and flat plate theory of Wilson,[33] which is close to Ref. 34. It must be noted that the present data was plotted without any transverse curvature correction. As previously stated, the turbulent heat transfer required no transverse curvature correction to agree with the empirical flat plate theory; thus, it seems possible, as a first approximation, to use the turbulent flat plate results for small angle sharp cones at high Mach numbers. Further experimental studies must be performed to verify this conclusion.

Another interesting observation is that the momentum Reynolds number, Re_θ, for fully turbulent flow decreases as the Mach number increases. At supersonic Mach numbers, Coles[35] found that $Re_\theta = 2000$ was sufficient for a turbulent

boundary layer while Hill[30] at a Mach number of about 9 found that the turbulent flow could exist down to Re_θ = 1500. The present work places the turbulent Re_θ down to approximately 1000.

Up to this point, only the effects of surface roughness on the sharp cone configuration have been discussed. It has been shown that the turbulent flow was obtained and that the surface roughness had a large effect in promoting turbulent boundary layer flow. Only one heat gage and Mach number location along the cone was used in the heat transfer discussion. Nevertheless, any gage or Mach number location could have been used with the arguments being exactly the same. Using the preceding discussion for the other five heat gage locations, the transition Reynolds numbers were determined for the corresponding Mach numbers. The results of this investigation are shown in Fig. 20 where the Reynolds number for the beginning and end of transition are plotted versus free stream Mach number. The other data[10,11,35,36] presented were obtained in continuous flow facilities under adiabatic wall conditions in comparison to the cool wall condition for the present data. As indicated, there is a decrease in the transition Reynolds number in the supersonic range after which it increases through the present range of data. For the smooth tip natural transition, the Reynolds number curve is still rising at M = 10.5 for both the beginning and end of transition. The question that is left to be answered is whether or not the transition Reynolds number curve continues to increase or bends over to some asymptotic value at higher Mach numbers. Further work is presently under way at the General Electric Research Laboratory to try to answer this question.

From Fig. 20 it is also possible to graphically observe the strong effect of surface roughness. The increment in Reynolds number between the beginning and end of transition is much less for the rough sharp tip than for the smooth tip cone. This effectively means that the surface roughness greatly shortens the transition region. The agreement of the adiabatic and cool wall conditions at a Mach number of about 8 indicates that the wall cooling effect for stabilizing the laminar boundary layer is small at high Mach numbers.

B. Effects of Tip Bluntness

With the sharp tip data as background information, it was then possible to study the effects of different types of tip bluntness. As before, the discussion of the heat transfer data will focus on the first heat transfer gage location. Referring to Fig. 1, the various tips will be designated as shown. The hemisphere and flat blunt tips have a diameter of 0.400 in. while the flat face of the rough blunt tip has a diameter of 0.072 in. The lowest reservoir condition used for the study of bluntness effects was that of T_5 = 1400°K and P_5 = 585 psia, Fig. 5. It is observed in this figure that the three types of bluntness, hemisphere, flat, and rough, gave the same results of laminar boundary layer flow with no significant difference in the magnitude. All the heat transfer magnitudes for bluntness are slightly above the smooth tip case. At this condition the Reynolds number was too low to separate the effects of the different tips on transition.

The next higher reservoir pressure studied was P_5 = 890 psia, Fig. 7. This figure was discussed previously, and it shows the rough sharp tip to be in turbulent flow, the smooth sharp tip to be in transition flow, and the hemisphere tip to be in laminar flow. The hemisphere tip gave a smooth heat trace which has been established as indicative of the laminar flow. From Fig. 7, it is evident that with the proper tip, it is possible to either delay or promote boundary layer transition.

In Fig. 8 a comparison of the three different tip bluntness are made. Actually due to the physical size of the tip bluntness, only the hemisphere and flat blunt tip can be compared directly while the rough blunt tip must more or less be compared to the rough sharp tip. In Fig. 8 it is observed that there is no significant difference between the hemisphere and flat blunt tip since they both indicate a laminar boundary layer with nearly the same local heat transfer magnitude. On the other hand, the rough blunt tip shows large oscillations as compared to the small oscillation for the rough sharp tip at the same reservoir condition. This would indicate the rough blunt tip to be in transition flow at the first heat gage location as compared to fully turbulent flow for the rough sharp tip. Therefore, all three types of blunt tips demonstrate that bluntness tends to delay boundary layer transition to some degree.

The hemisphere tip was tested at higher reservoir pressures in order to obtain some information regarding the incremental increase in the transition Reynolds number due to bluntness. At a reservoir pressure of 1300 psia, the hemisphere tip gave transition flow at the first heat gage, Fig. 9. The hemisphere was still in transition flow at

P_5 = 2200 psia which was the highest reservoir pressure tested, Fig. 11. This is the correct trend since it required a P_5 = 2200 psia to put the smooth sharp tip configuration in fully turbulent flow. The incremental increase in the beginning transition Reynolds number for the hemisphere tip over the sharp tip is $\Delta Re_{tr} = 1.4 \times 10^6$ which is about a 35 percent increase for a cone base diameter to tip diameter ratio of 20. This percentage increase is in the same range as indicated by Brinich and Sands[37] for bluntness effects on 10° cone boundary layer transition at a Mach number of 3.1.

C. Effects of Angle of Attack

The angle of attack data was obtained by pitching the model to plus and minus two degrees while holding the cone tip on the nozzle axis. Cone surface pressure and local heat transfer data were obtained for both configurations. The pressure and heat gages remained in the vertical plane with respect to the pitch axis. The pressure data indicated that the various configurations did not significantly affect the basic nozzle flow. It also indicated that there was no boundary layer separation on the sheltered side of the model. Three reservoir pressures at a stagnation temperature of 1400°K were used in this preliminary angle of attack study: P_5 = 450 psia, P_5 = 585 psia, and P_5 = 1300 psia. Only the smooth sharp tip was used which leaves the surface roughness and bluntness effects for further study.

Typical oscilloscope traces for one heat transfer gage are presented in Fig. 21. The plus angle of attack is taken to be with the heat gages on the sheltered side of the cone and the minus angle of attack to be with the heat gages on the windward side. Considering the 450 psia

reservoir pressure, the $\alpha = 0°$ trace is very smooth while the $\alpha = +2°$ trace shows sizeable oscillations which are indications of transition flow. At the $P_5 = 1300$ psia condition, the $\alpha = -2°$ condition is in the early stages of transition, the $\alpha = 0°$ condition is well into transition, and the $\alpha = +2°$ condition consists of small high frequency oscillations which are typical of turbulent flow. From these heat transfer traces, it is already evident that the cross flow, due to the angle of attack, is very effective in controlling the type of boundary layer generated.

The local heat transfer distributions for both angles of attack are presented in Figs. 22 to 27. The curves in these figures were calculated by using the previous zero angle of attack theories, the $\pm 2°$ cone surface pressure distributions, and the work of Reshotko.[38] The first three figures in the series contain the $+2°$ results, heat gages on the sheltered side of the cone. Focusing on the first heat gage location, the reservoir pressure of 450 psia, Fig. 22, placed this location in transition flow where before at zero angle of attack it gave smooth laminar boundary layer flow, Fig. 4. The 585 psia reservoir pressure still locates the first heat gage in transition flow, but the magnitude has increased toward the turbulent theory, Fig. 23. The 1300 psia reservoir pressure, Fig. 24, shows the heat transfer to have small oscillations with the magnitude close to that of the turbulent theory; hence, the conclusion would be that turbulent boundary layer flow exists for $+2°$ angle of attack at this pressure. The Reynolds number at this location and pressure is approximately 5×10^6. This points out that the cross flow has destabilized the laminar boundary layer to the extent of

reducing the end of transition Reynolds number by approximately 60 percent on the sheltered side of the cone over that of the zero angle of attack.

The minus angle of attack data is presented in Figs. 25 to 27. From Fig. 25, the 450 psia reservoir pressure condition gave smooth heat traces with no oscillations which are characteristics of the laminar flow. The deviation between the experimental data and laminar theory is about the same as for the zero angle of attack case. The actual heat transfer magnitude is greater than for the corresponding $\alpha = 0°$ due to the cross flow effect on the windward side. The results for the 585 psia reservoir pressure, Fig. 26, are similar to the 450 psia pressure with the boundary layer remaining laminar. The 1300 psia reservoir condition presents a different picture in that oscillations are present in the heat gage traces, and the heat transfer magnitude is approaching the turbulent value. This particular situation is that of transition flow with a Reynolds number of 6×10^6 at the first heat gage. This is a delay in the beginning of transition on the windward side with approximately a 60 percent increase in Reynolds number above that of the zero angle of attack. Thus, the windward most boundary layer changed from laminar to transition as the reservoir pressure increased from 450 psia to 1300 psia.

With respect to $\alpha = 0°$, the cross flow for $\alpha = 2°$ caused the transition to move forward on the sheltered side of the cone and rearward on the windward side. This result is in agreement with the free-flight data of Jedlicka, Wilkins, and Seiff[12] at a Mach number of 3.5. The significance of this result applies to the re-entry nose cone flying at varying angles of attack. As demonstrated, the cross flow at angle of

attack will cause the transition point to oscillate along the body surface which in turn will affect the body wake. Some vehicles might have a completely laminar boundary layer and wake at zero angle of attack while at some other angle of attack, the transition of the boundary layer may occur and change the wake characteristics with a corresponding change in the ground radar image.

V. CONCLUSIONS

The laminar boundary layer transition on a 10° cone was investigated in a shock tunnel over the Mach number range of 8.5 to 10.5. The stagnation temperature for all the tests was approximately 1400°K which gave a nearly perfect gas flow. Therefore, the Reynolds number was varied at any given cone location by simply varying the reservoir pressure.

Only the effects of Mach number, surface roughness, tip bluntness, and 2° angle of attack on the boundary layer transition were investigated. Surface heat transfer gages were the primary instruments used to locate the beginning and end of the transition region. These gages had a response time of a few microseconds which enabled them to detect the turbulent bursts as they crossed the gages. It was further demonstrated in this report that the transition of the hypersonic laminar boundary layer starts with the appearance of turbulent spots or bursts in the same manner as for subsonic transition. Schlieren photographs and a pitot tube boundary layer survey were used to verify the interpretation of the local heat transfer data. The measured cone surface pressure data were used to check the basic nozzle flow and determine the flow properties just outside the boundary layer.

The natural boundary layer transition for the smooth sharp tip had a long transition region with the beginning and end transition Reynolds numbers of 3.8 $x10^6$ and 9.6 $x10^6$ for the 8.5 Mach number location. On the other hand, the beginning and end transition Reynolds numbers were 2.2 $x10^6$ and 4.2 $x10^6$ at the same location for the rough sharp tip which demonstrates the effectiveness of proper tip surface roughness in promoting transition. Surface cooling indicated no particular stabilizing effect on the laminar boundary layer when compared to the adiabatic wall condition at hypersonic Mach numbers.

The schlieren results gave visual evidence of the start of transition with the burst formation followed by laminar flow. They also presented turbulent flow as having a waffle type appearance as would be expected since the turbulent action would tend to smooth out the steep density gradients of the hypersonic laminar boundary layer at the outer edge.

The boundary layer pitot tube survey was conducted at a Mach number of 10 location. The total pressure profiles showed a large difference between the laminar and turbulent flows. The transition flow had large oscillations especially towards the outer edge of the boundary layer. This maximum oscillation layer agreed with the heat gage results which indicated the turbulent bursts to be moving at approximately 0.9 of the free-stream velocity. The critical layer, point of maximum oscillation, is thus well removed from the wall at the present hypersonic conditions which would help to explain why the wall cooling effect for stabilization is small.

The velocity, temperature, and density profiles determined from the impact data were the same for both the natural and roughness induced turbulent boundary layer which indicates that the boundary layer flow does not have a past history once it is turbulent. The skin friction data obtained from the velocity profiles correlated very well with the heat transfer data through the Reynolds analogy. The turbulent skin friction and heat transfer data agreed reasonably well with the corresponding flat plate emperical theories without any transverse curvature correction which implies that no such correction is necessary at high Mach numbers. This particular implication must be checked further experimentally for verification at high Mach numbers.

The bluntness results demonstrated that the tip bluntness delays transition over that of the sharp tip configuration for both the smooth and rough case. There was no significant difference between the hemisphere blunt tip and flat blunt tip configuration for the reservoir conditions tested. The incremental increase in the beginning transition Reynolds number due to the hemisphere was 1.4×10^6 for a bluntness ratio of 20. Further investigations must be conducted to determine the ΔRe_{tr} as a function of bluntness ratio at high Mach numbers.

The 2° angle of attack data pointed out the strong influence of the cross flow on the boundary layer. The end of transition Reynolds number decreased by 60 percent on the sheltered side of the model as compared to that of the zero angle of attack while the beginning transition Reynolds number increased by 60 percent on the windward side.

As a result, the cross flow promotes transition on the sheltered side and delays it on the windward side. Further study must be done to determine the effects of bluntness and surface roughness combined with angle of attack on the transition of the hypersonic laminar boundary layer.

ACKNOWLEDGMENTS

The support of A. J. Nerad contributed to the attainment of results presented in this paper. K. H. Cary and L. A. Osburg assisted with the instrumentation and mechanical design.

References

1. Tollmien, W., "Ein Allgemeines Kriterium der Instabilität Laminarer Gesihwindigkeitsverteilungen," Ges. Wiss. Göttingen Math. Phys. Klasse, Fachgruppe I, 1, 79-114 (1935); Engl. transl. in NACA Tech. Memo. No. 792 (1936).

2. Schlichting, H., Boundary Layer Theory, McGraw-Hill Book Co., New York (1960).

3. Lin. C.C., The Theory of Hydrodynamic Stability, Cambridge University Press, Cambridge, England (1955).

4. Lees, L., "The Stability of the Laminar Boundary Layer in a Compressible Fluid," NACA, TR 876 (1947).

5. Lees, L. and Reshotko, E., "Stability of the Compressible Laminar Boundary Layer," Jour. of Fluid Mech., Vol. 12, No. 4, pp. 555-590 (1962).

6. Laufer, J. and Verbalovich, T., "Stability and Transition of a Supersonic Boundary Layer," Jour. of Fluid Mech., Vol. 9, Part 2, pp. 257-299 (October 1960).

7. Demetriades, A., "An Experimental Investigation of the Stability of the Hypersonic Laminar Boundary Layer," Jour. Aero. Sci., Vol. 25, No. 9, pp. 579-600 (September 1958).

8. Schubauer, G. B. and Skramstad, H.K., "Laminar Boundary Layer Oscillations and Transition on a Flat Plate," NACA, TR909 (1948).

9. Schubauer, G.B. and Klebanoff, P.S., "Contributions on the Mechanics of Boundary Layer Transition," NACA, TN3489 (September 1955).

10. Klebanoff, P.S., Tidstrom, K.D., and Sargent, L.M., "The Three-Dimensional Nature of Boundary Layer Instability," Jour. of Fluid Mech., Vol. 12, No. 1, pp. 1-34 (1962).

11. Potter, J.L. and Whitfield, J.D., "Effects of Slight Nose Bluntness and Roughness on Boundary Layer Transition in Supersonic Flows," Jour. of Fluid Mech., Vol. 12, No. 4, pp. 508-535 (1962).

References (continued)

12. Jedlicka, J.R., Wilkins, M.E., and Seiff, A., "Experimental Determination of Boundary Layer Transition on a Body of Revolution," NACA, TN 3342, (October 1954).

13. Lyons, W.C., Jr. and Sheetz, N.W., Jr., "Free Flight Experimental Investigations of the Effects of Boundary Layer Cooling on Transition," U.S. Naval Ord. Lab., Rep. 61-83 (September 1961).

14. Levensteins, Z.J., "Hypersonic Wake Characteristics Behind Sphere and Cones," Naval Ord. Lab. Publ. (August 1963).

15. Nagamatsu, H.T., and Sheer, R.E., Jr., "Boundary Layer Transition on a Highly Cooled 10° Cone in Hypersonic Flows," General Electric Research Lab. Rep. No. 64-RL-(3622C) (1964).

16. Nagamatsu, H.T., Graber, B.C., and Sheer, R.E., Jr., "Transition of Hypersonic Boundary Layer," General Electric Research Lab. Rep. No. 64-RL-(3692C) (1964).

17. Nagamatsu, H.T., Geiger, R.E., and Sheer, R.E., Jr., "Hypersonic Shock Tunnel," Jour. ARS 29, 332-340 (1959).

18. Nagamatsu, H.T., Weil, J.A., and Sheer, R.E., Jr., "Heat Transfer to Flat Plate in High Temperature Rarefied Ultrahigh Mach Number Flow," Jour. of ARS, Vol. 32, No. 4,pp. 533-541 (April 1962).

19. Nagamatsu, H.T., Workman, J.B., and Sheer, R.E., Jr., "Hypersonic Nozzle Expansion with Air Atom Recombination Present", J. Aero. Sci., 28, 833 (1961).

20. Nagamatsu, H.T., and Sheer, R.E., Jr., "Vibrational Relaxation and Recombination of Nitrogen and Air in Hypersonic Nozzle Flows", AIAA Preprint No. 64-38 (1964).

21. Gilmore, F.R., "Equilibrium Composition and Thermodynamic Properties of Air to 24,000°K," Rand Rept. RM-1543 (1953).

22. Hirschfelder, J.D., and Curtiss, C.F., "Thermodynamic Properties of Air," Univ. of Wisconsin, CM-518, Navy Bu. Ord. Contract No. 9938 (1948).

23. Feldman, S., "Hypersonic Gas Dynamic Charts for Equilibrium Air," AVCO Res. Lab. Rept. (Jan. 1957).

References (continued)

24. Weil, H., "Effects of Pressure Gradient on Stability and Skin Friction in Laminar Boundary Layers in Compressible Fluids," Jour. Aero. Sci., Vol. 18, No. 5, pp. 311-318 (May 1951).

25. Howarth, L., Modern Developments in Fluid Dynamics High Speed Flow, 1, p. 402, Oxford University Press, London (1953).

26. Persh, J., "An Analytical Investigation of Turbulent Boundary Layer Heat Transfer Coefficients for Supersonic and Hypersonic Flow," Navord Report 4099, (Oct. 1955).

27. Lobb, K.R., Winkler, E.M., and Persh, J., "Experimental Investigation of Turbulent Boundary Layers in Hypersonic Flow", Navord Report 3880, (Marcy 1955).

28. Champan, D.R., and Kester, R.H., "Measurements of Turbulent Skin Friction on Cylinders in Axial Flow at Subsonic and Supersonic Velocities," Jour. Aero. Sci., Preprint No. 391 (Jan. 1953).

29. Brinich, P.F., and Diaconis, N.A., "Boundary Layer Development and Skin Friction at Mach Number 3.05," NACA TN 2742 (July 1952).

30. Hill, F.K., "Boundary Layer Measurements in Hypersonic Flow", Jour. of Aero. Sci. 23, No. 1, pp. 35-43, (1956).

31. von Kármán, T., "Turbulence and Skin Friction," Jour. Aero. Sci., Vol. 1, No. 1, pp. 1-20 (January 1934).

32. Van Driest, E.R., "The Turbulent Boundary Layer for Compressible Fluids on a Flat Plate with Heat Transfer," North American Aviation, Inc., Rep. AL-1006, (Feb. 1950).

33. Wilson, R.E., "Turbulent Boundary Layer Characteristics at Supersonic Speeds -- Theory and Experiment," Jour. of Aero. Sci., 17, No. 9, pp. 585-594, (Sept. 1950).

34. Persh, J., "A Theoretical Investigation of Turbulent Boundary Layer Flow with Heat Transfer at Supersonic and Hypersonic Speeds", Navord Report 3854.

35. Coles, D., "Measurements of Turbulent Friction on a Smooth Flat Plate in Supersonic Flows," Jour. of Aero. Sci., 21, No. 7, (July 1954).

References (continued)

36. Korkegi, R.H., "Transition Studies and Skin Friction Measurements on an Insulated Flat Plate at a Mach Number of 5.8", Jour. of Aero. Sci., 23, No. 2, pp. 97-108, (Feb. 1956).

37. Brinich, P.F., and Sands, N., "Effects of Bluntness on Transition for a Cone and a Hollow Cylinder at Mach 3.1", NACA, TN 3979, (May 1957).

38. Reshotko, E., "Laminar Boundary Layer with Heat Transfer on a Cone at Angle of Attack in a Supersonic Stream," NACA, TN 4152, (December 1957).

SMOOTH SHARP

ROUGH SHARP

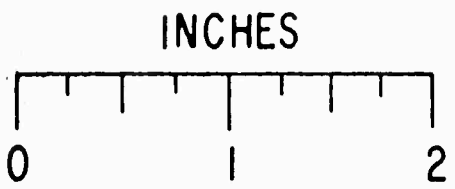

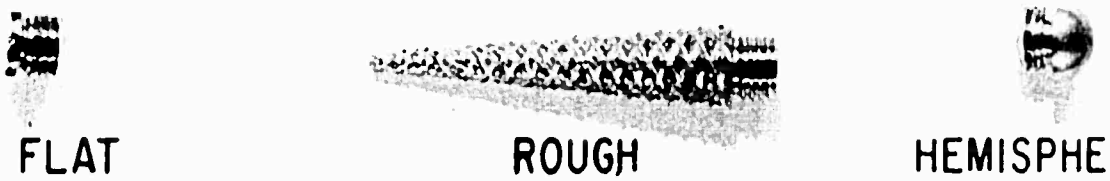

FLAT BLUNT

ROUGH BLUNT

HEMISPHERE BLUNT

Fig. 1 Interchangeable tips for 10° cone model.

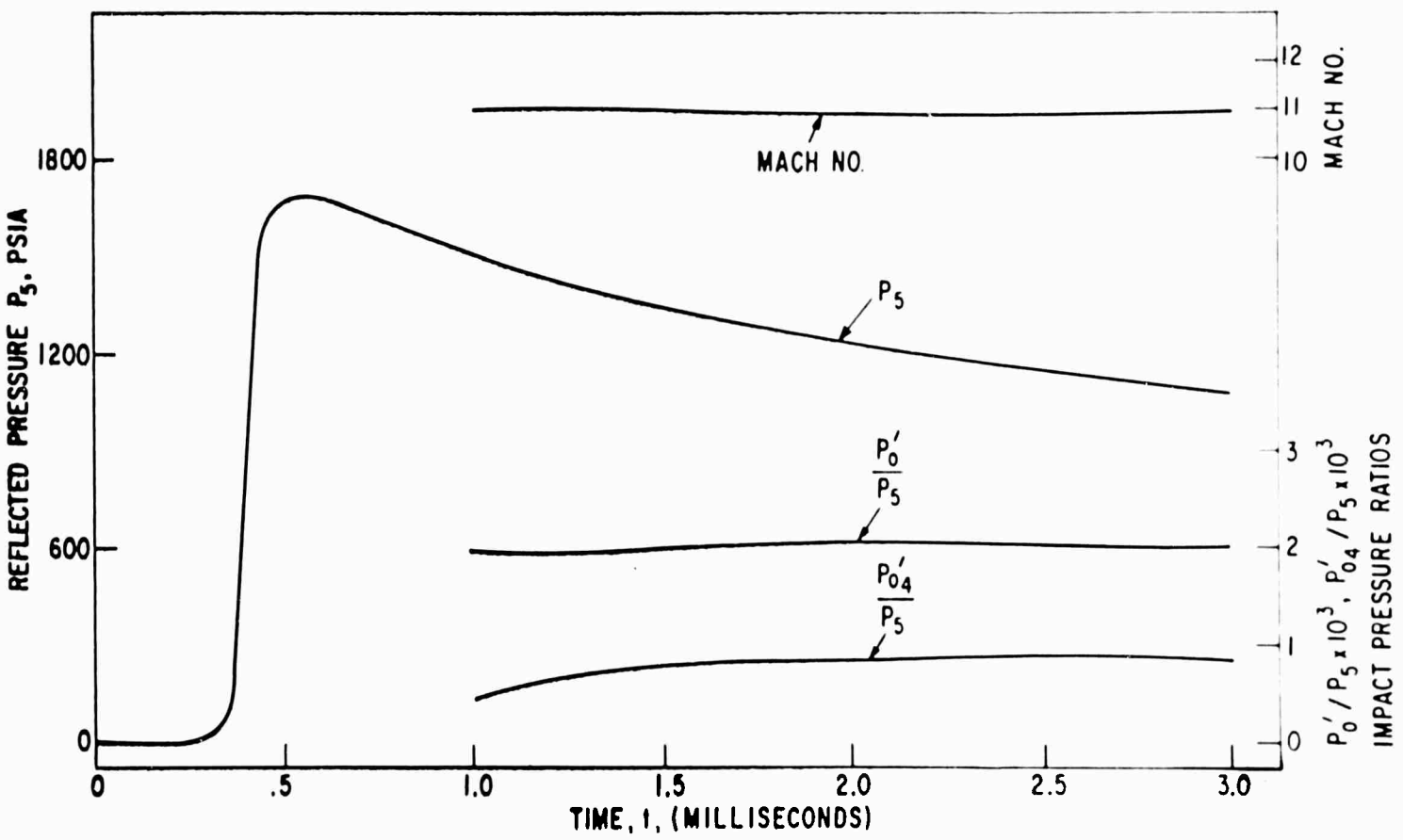

Fig. 2 Variation of reflected pressure, free stream impact pressure ratio, typical boundary layer impact pressure ratio, and Mach number with time.

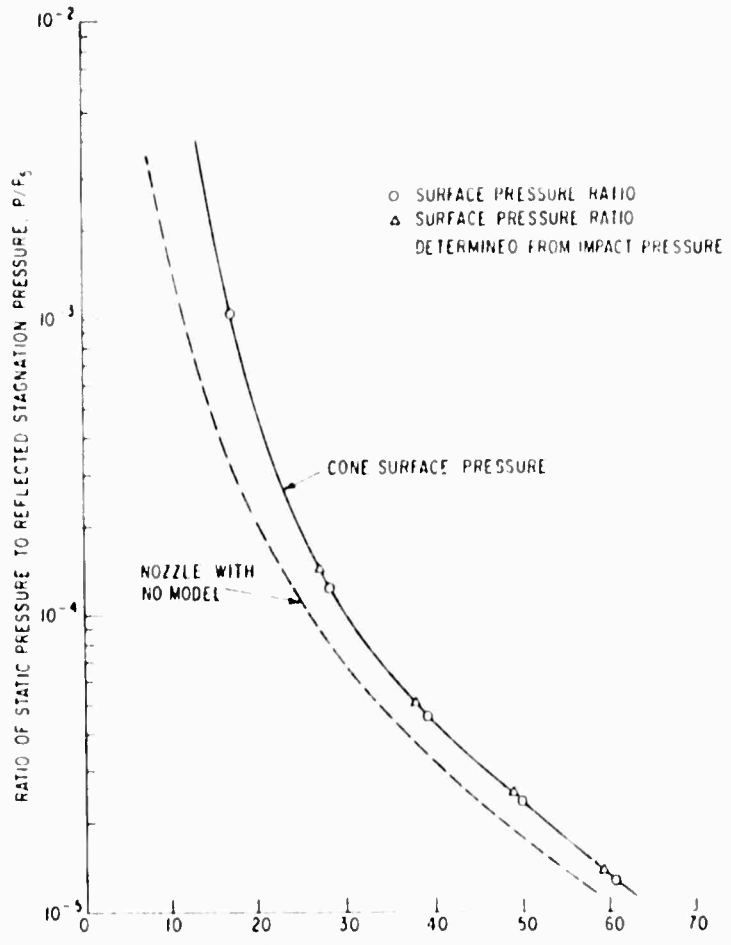

Fig. 3 Static pressure distribution for 10° cone in hypersonic nozzle with reflected stagnation pressure P_5 = 1300 psia, and temperature T_5 = 1400°K.

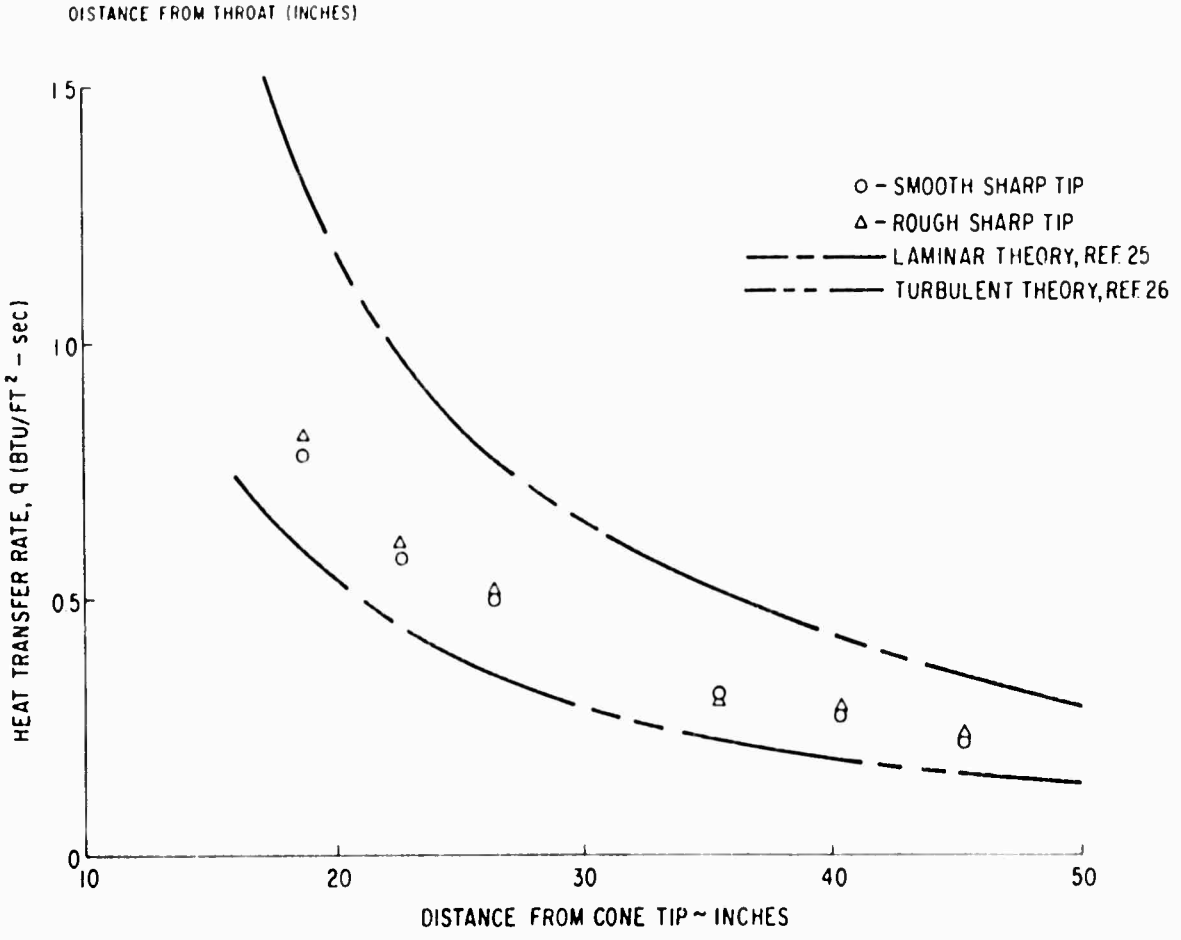

Fig. 4 Heat transfer distribution for different cone tips at reservoir pressure P_5 = 450 psia, and temperature T_5 = 1400°K.

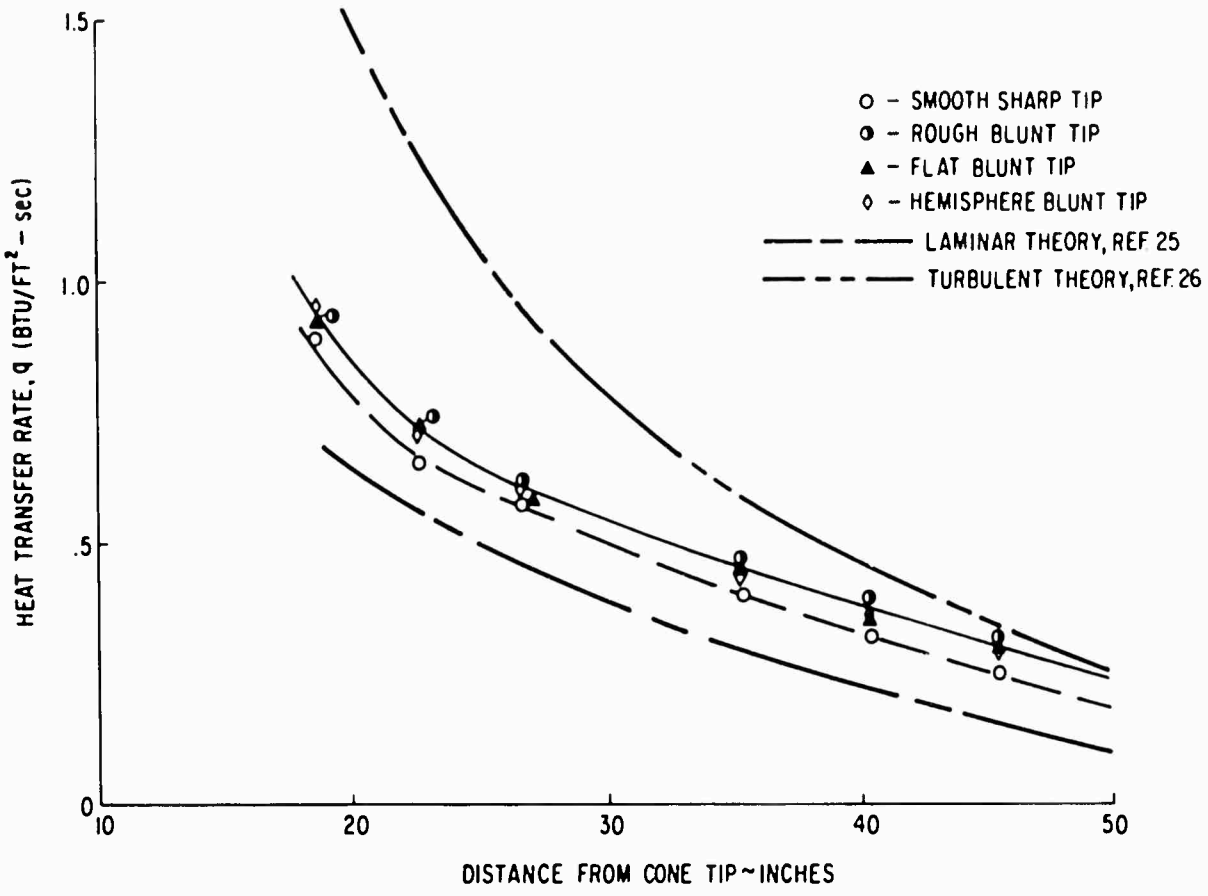

Fig. 5 Heat transfer distribution for different cone tips at reservoir pressure P_5 = 585 psia, and temperature T_5 = 1400°K.

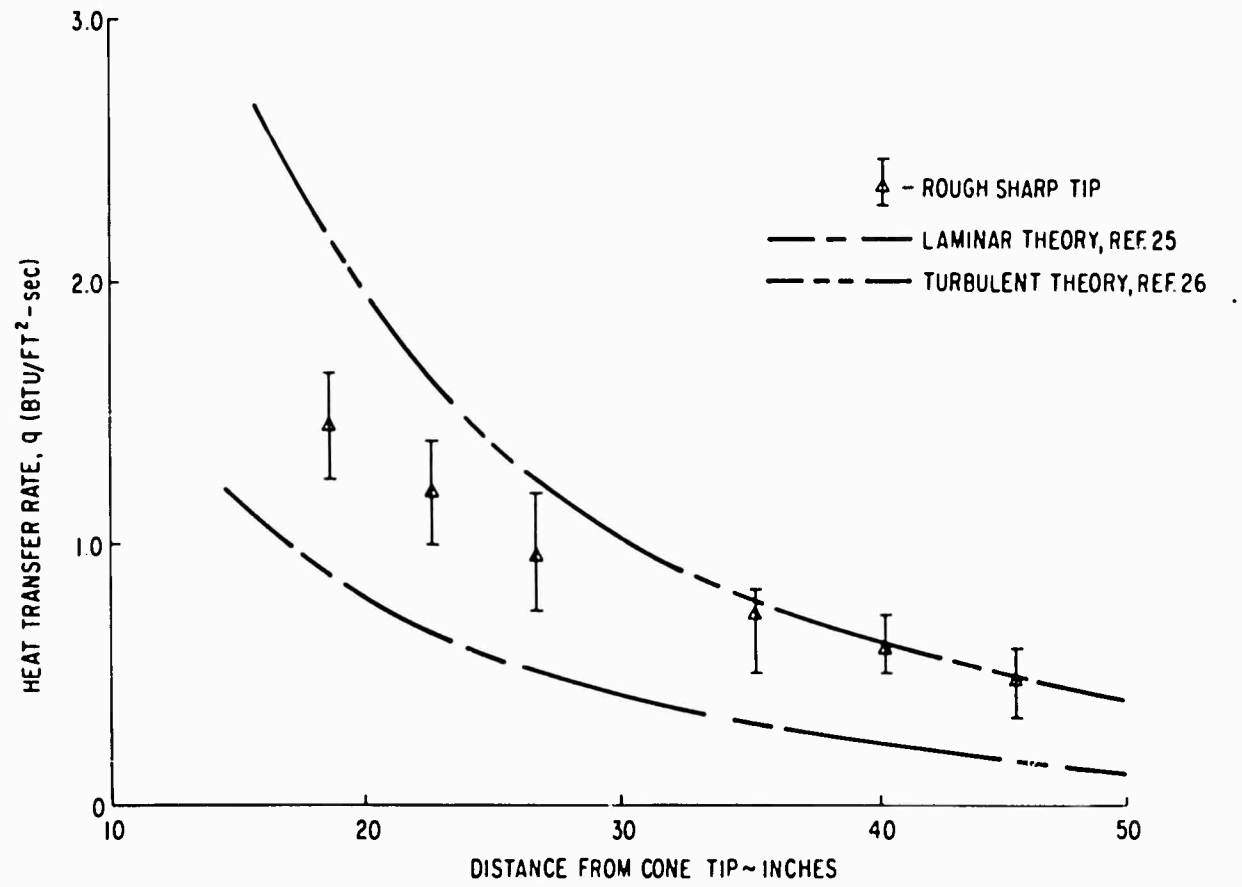

Fig. 6 Heat transfer distribution at reservoir pressure P_5 = 760 psia, and temperature T_5 = 1400°K.

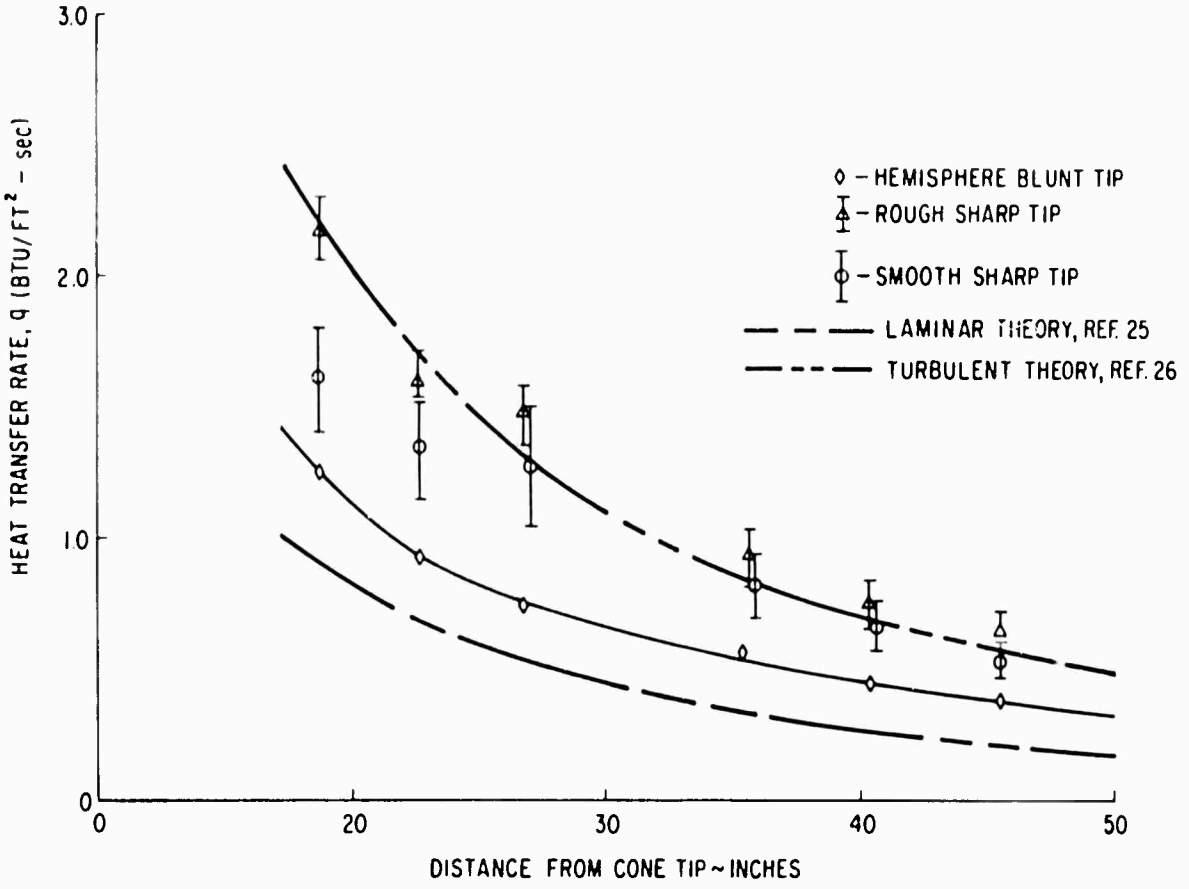

Fig. 7 Heat transfer distribution for different cone tips at reservoir pressure P_5 = 890 psia, and temperature T_5 = 1400°K.

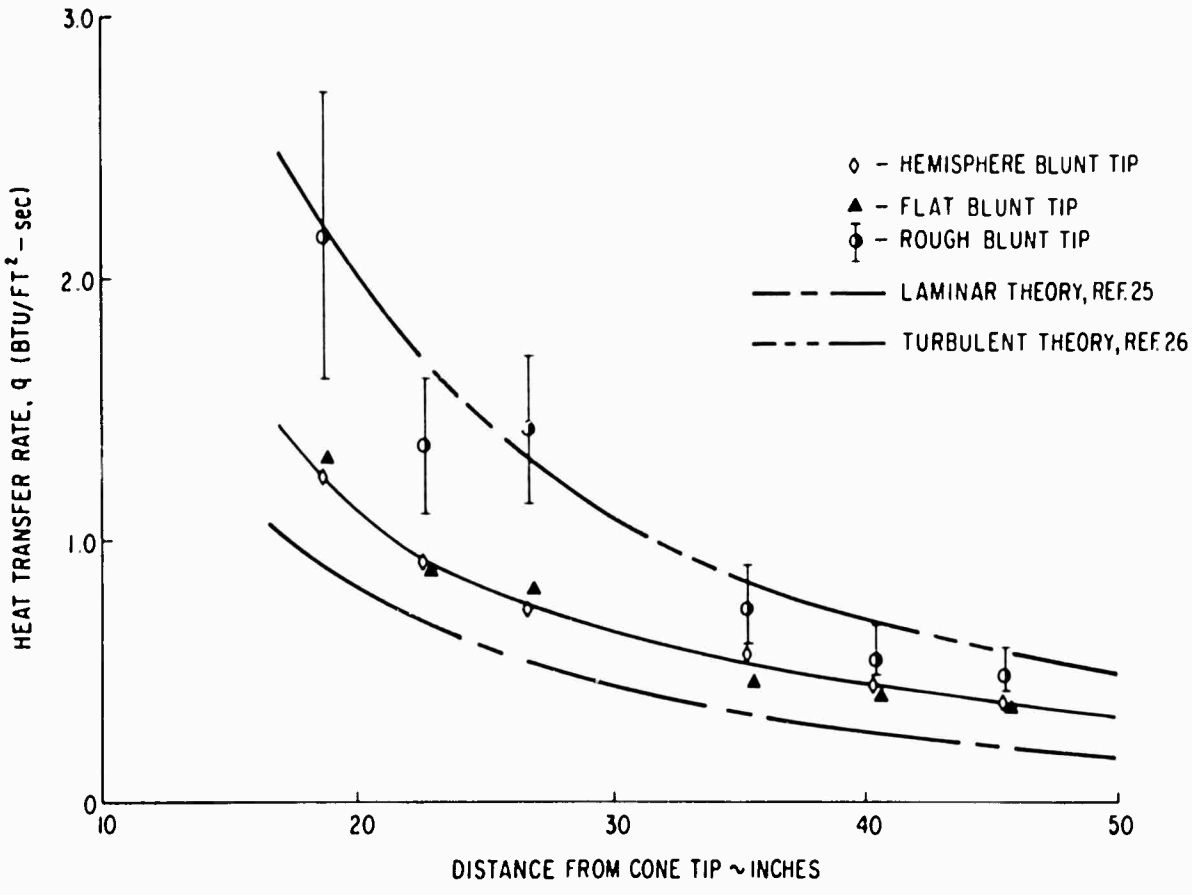

Fig. 8 Heat transfer distribution for different cone tips at reservoir pressure P_5 = 890 psia, and temperature T_5 = 1400°K.

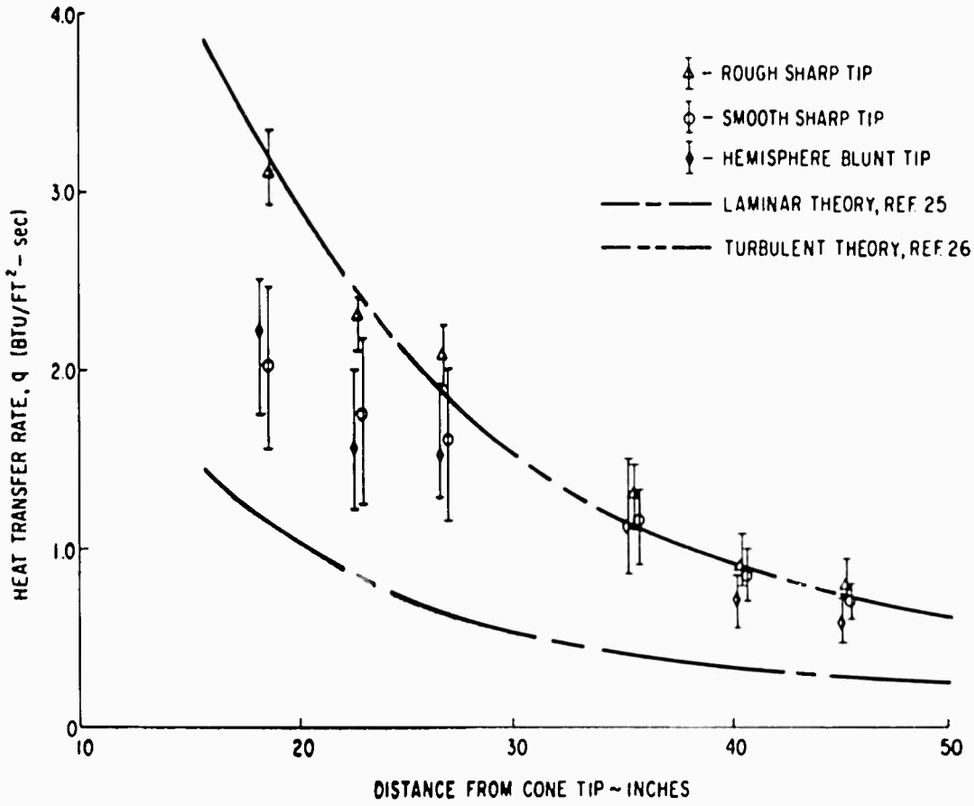

Fig. 9 Heat transfer distribution for different cone tips at reservoir pressure P_5 = 1300 psia, and temperature T_5 = 1400°K.

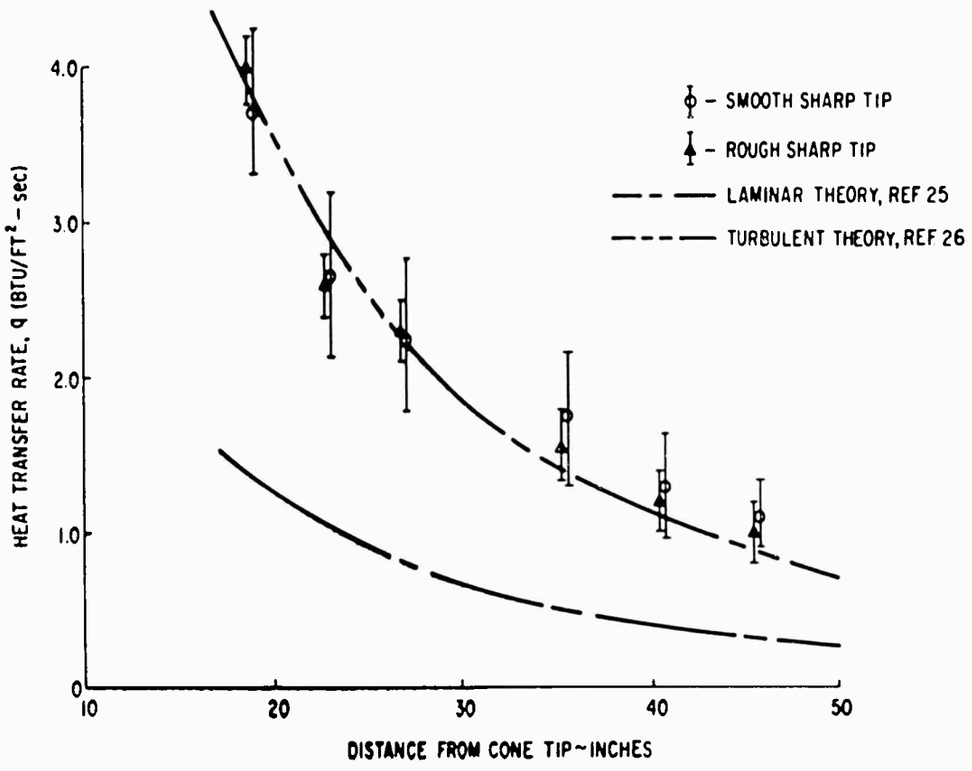

Fig. 10 Heat transfer distribution for different cone tips at reservoir pressure P_5 = 1800 psia, and temperature T_5 = 1400°K.

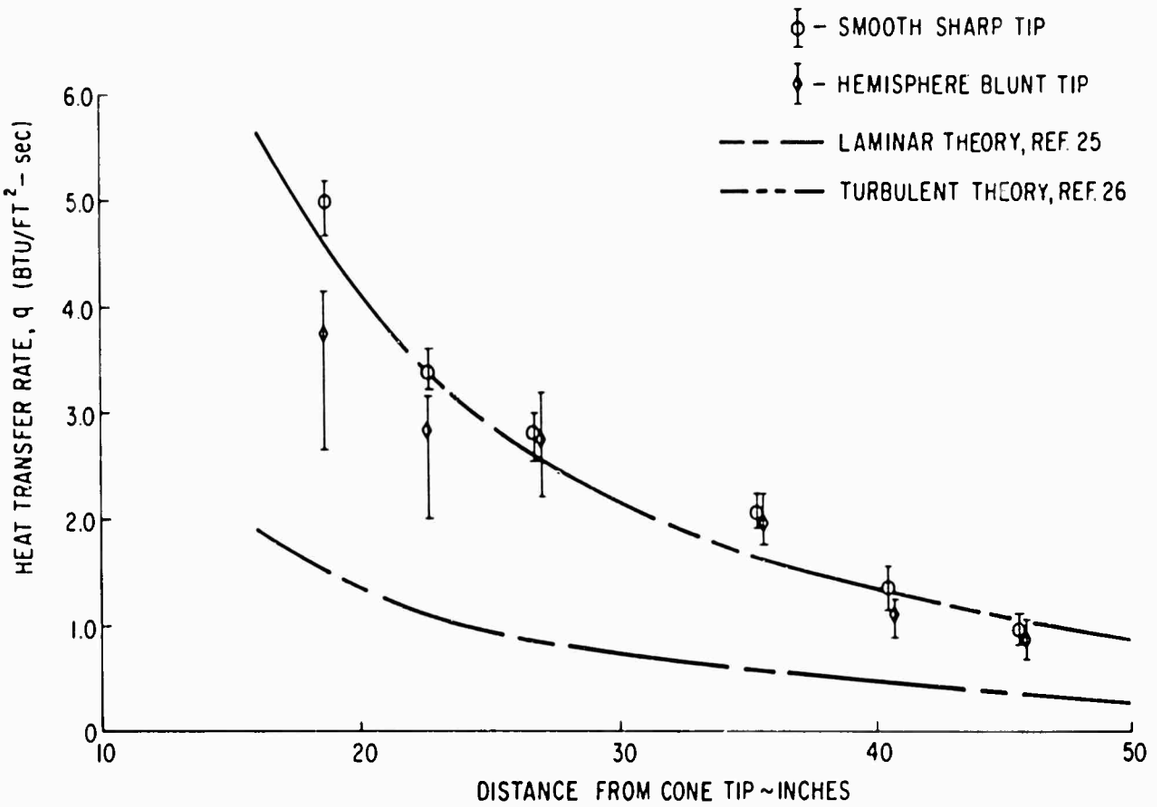

Fig. 11 Heat transfer distribution for different cone tips at reservoir pressure P_5 = 2200 psia, and temperature T_5 = 1400°K.

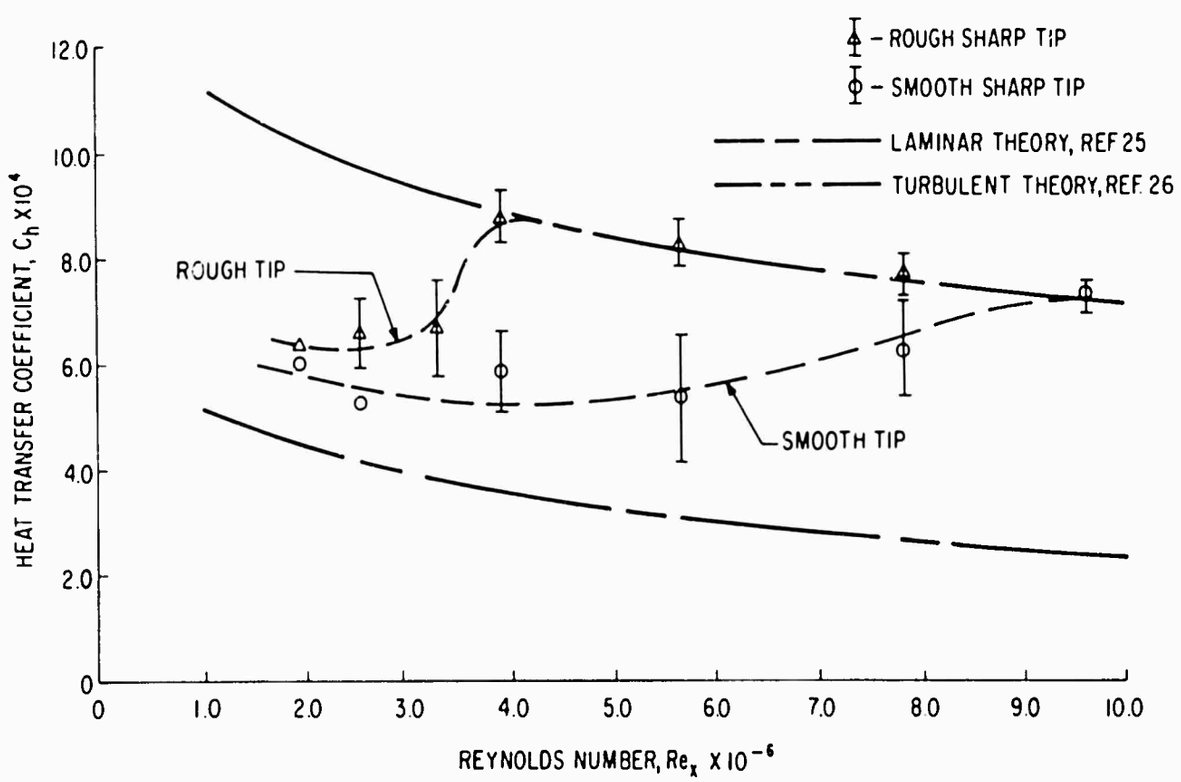

Fig. 12 Variation of local heat transfer coefficient with surface Reynolds number for different cone tips at M = 8.5.

Fig. 13 Composite schlieren photographs of flow over a 10° cone with smooth sharp (top) and rough sharp (bottom) tips for reservoir pressure P_5 = 1300 psia, and temperature, T_5 = 1400°K.

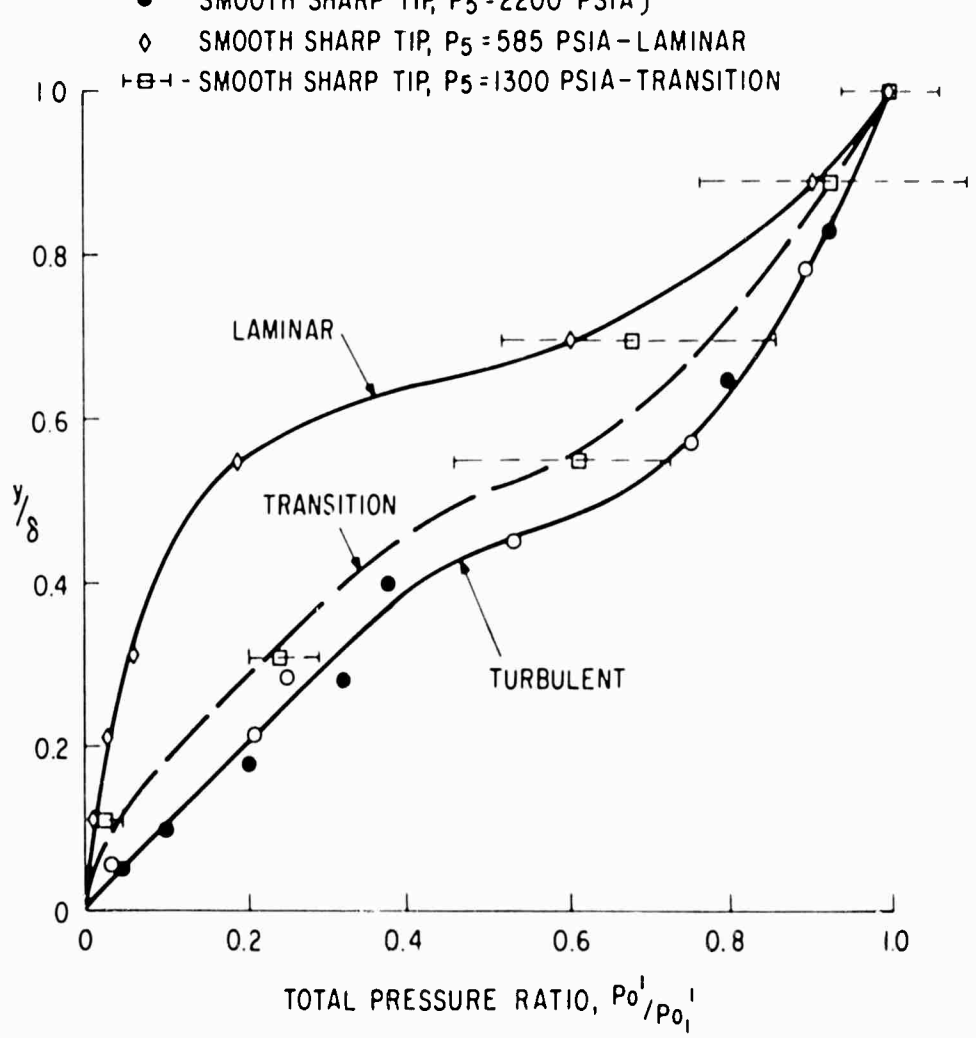

Fig. 14 Nondimensional impact pressure profiles for various types of boundary layers T_5 = 1400°K, $M_1 \approx 10$.

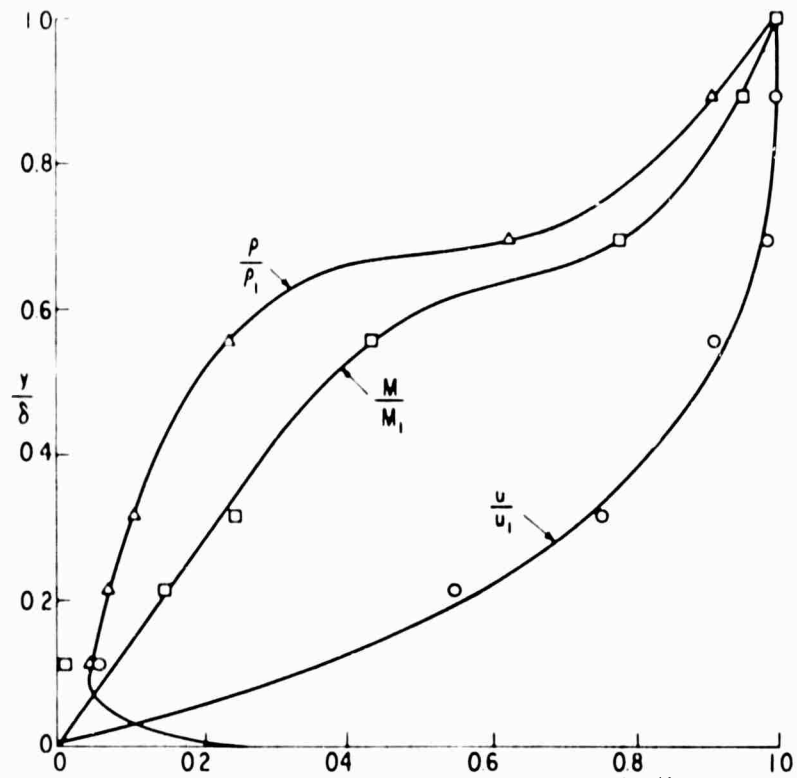

Fig. 15 Nondimensional laminar boundary layer profiles (smooth tip) $P_5 = 585$ psia, $T_5 = 1400°K$, $M_1 \approx 10$.

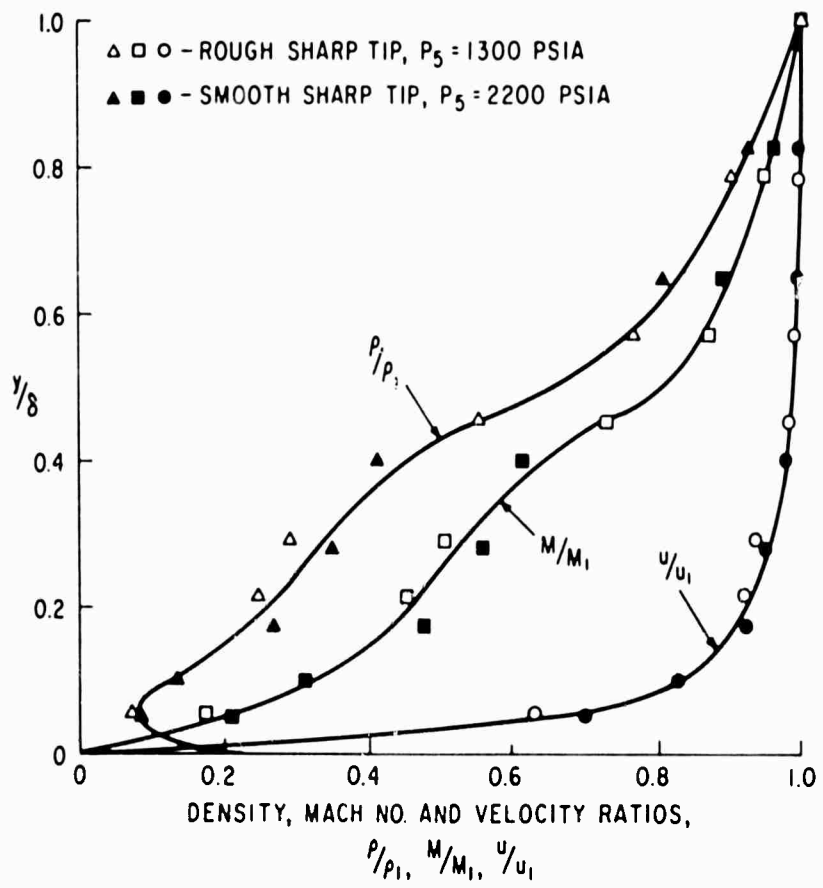

Fig. 16 Nondimensional turbulent boundary layer profiles $T_5 = 1400°K$, $M_1 \approx 10$.

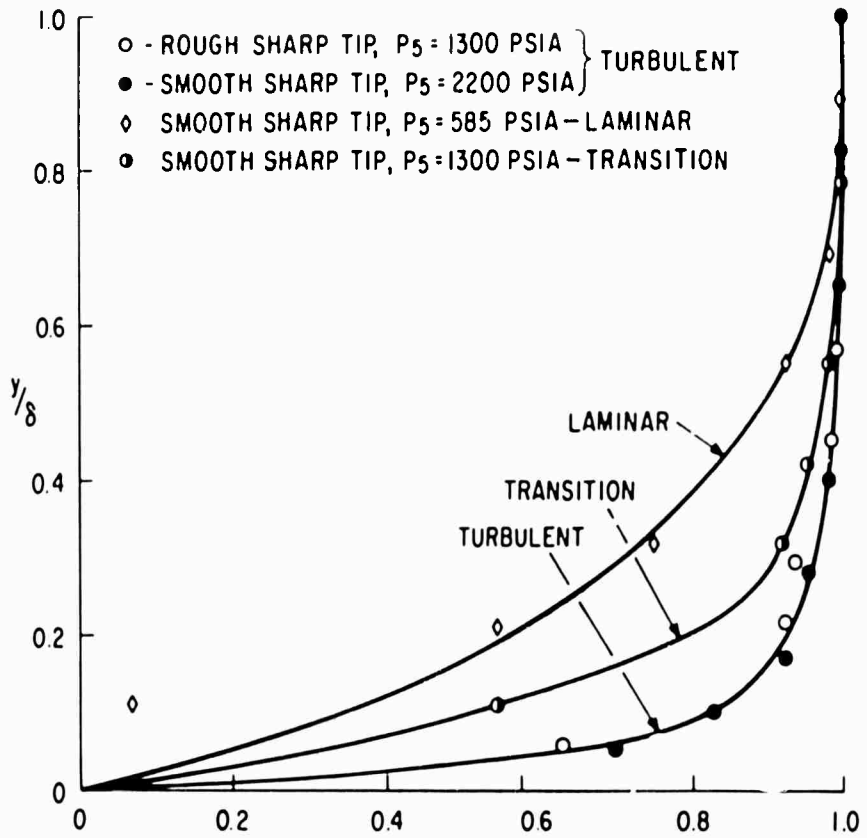

Fig. 17 Nondimensional velocity profiles for various types of boundary layers $T_5 = 1400°K$, $M_1 \approx 10$.

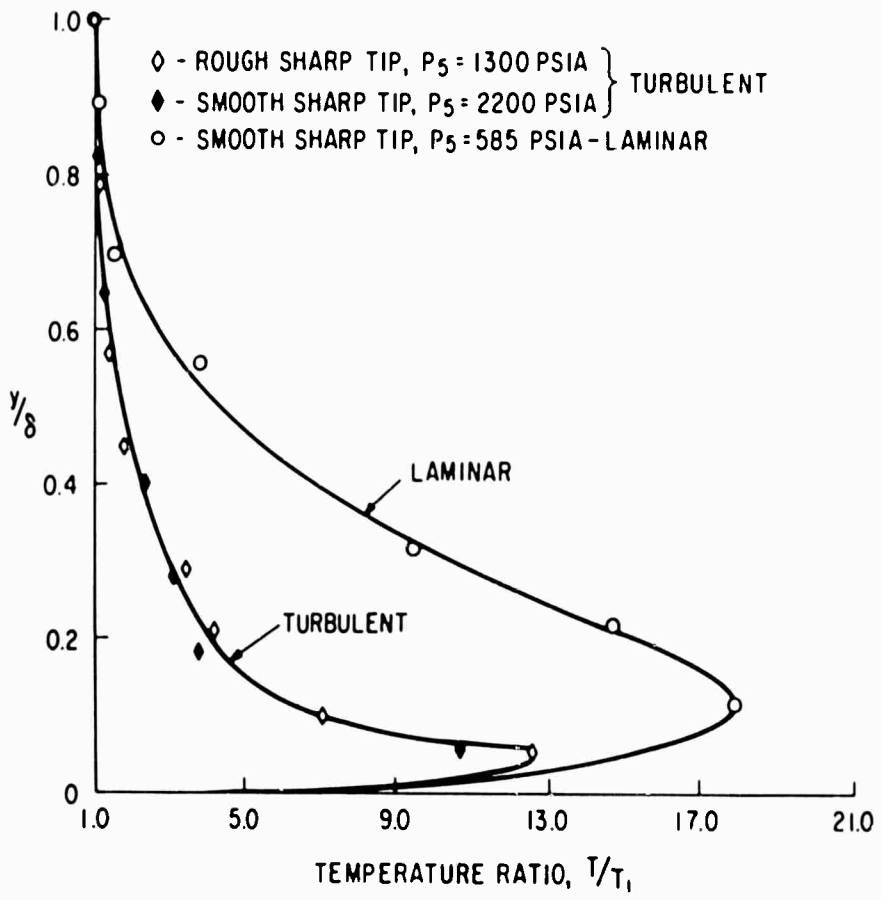

Fig. 18 Nondimensional temperature profiles for various types of boundary layers $T_5 = 1400°K$, $M_1 \approx 10$.

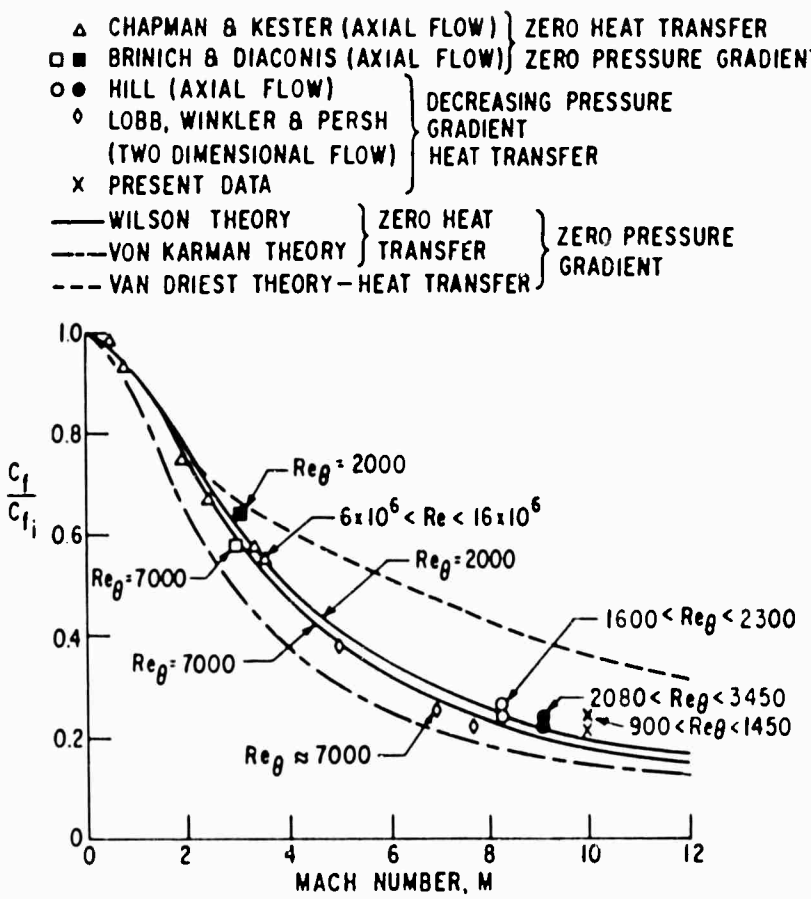

Fig. 19 Turbulent skin friction ratio vs free stream Mach number.

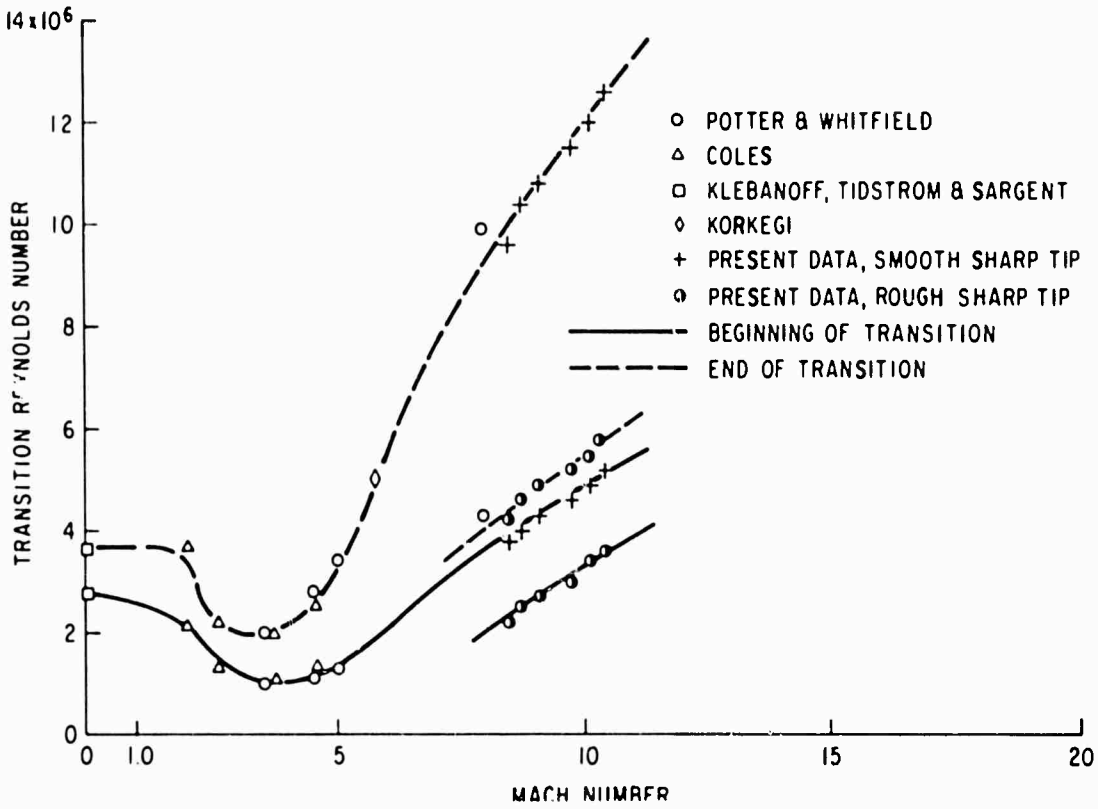

Fig. 20 Comparison of transition Reynolds number as a function of Mach number for different flow facilities.

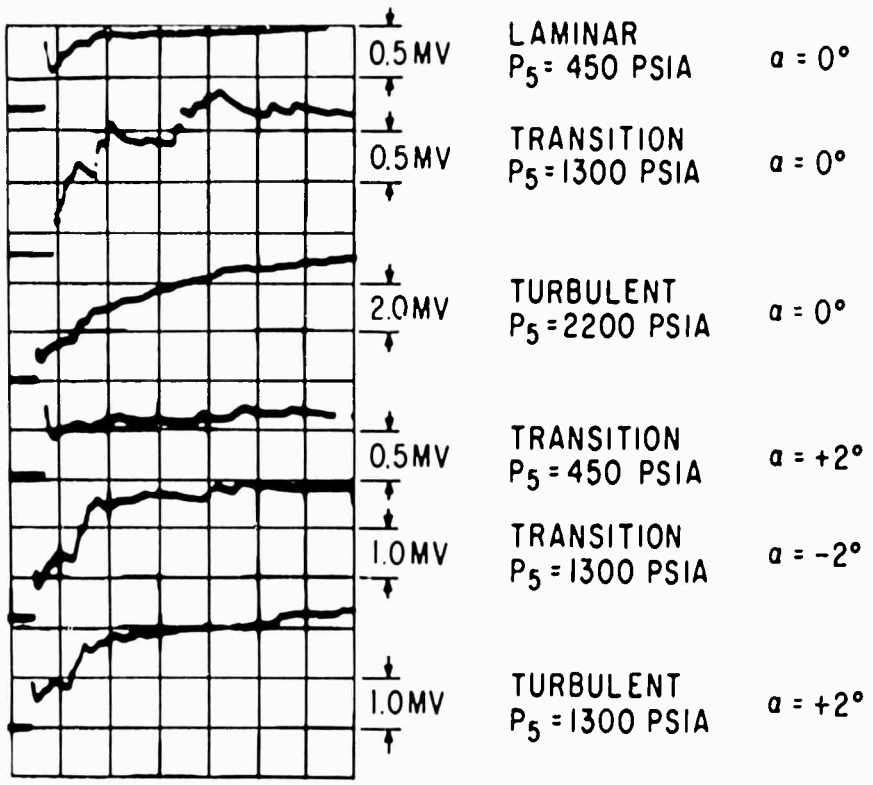

Fig. 21 Typical heat transfer traces for smooth sharp tip and varying angles of attack: T_5 = 1400°K.

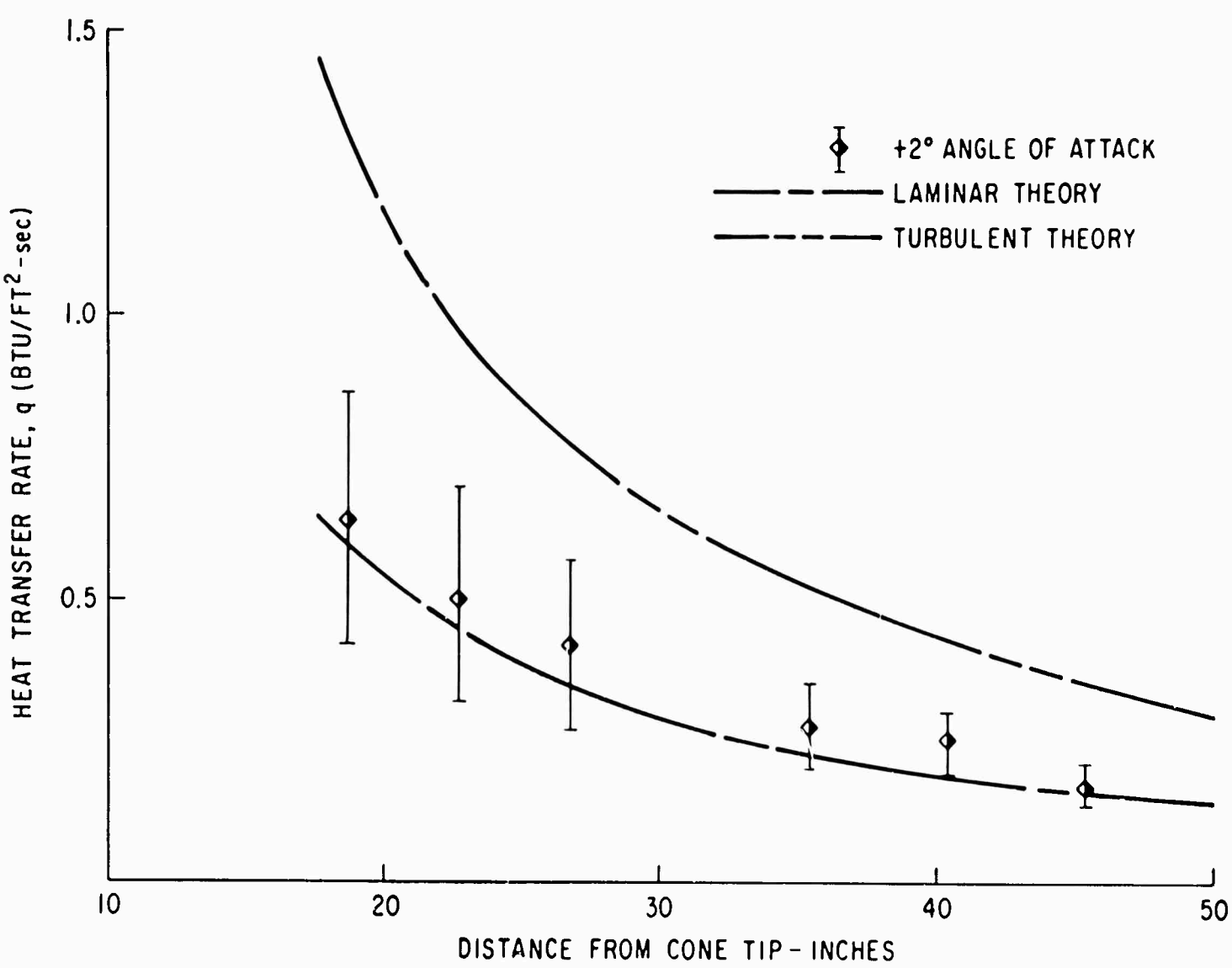

Fig. 22 Heat transfer distribution for smooth tip cone at +2° angle of attack: P_5 = 450 psia, T_5 = 1400°K.

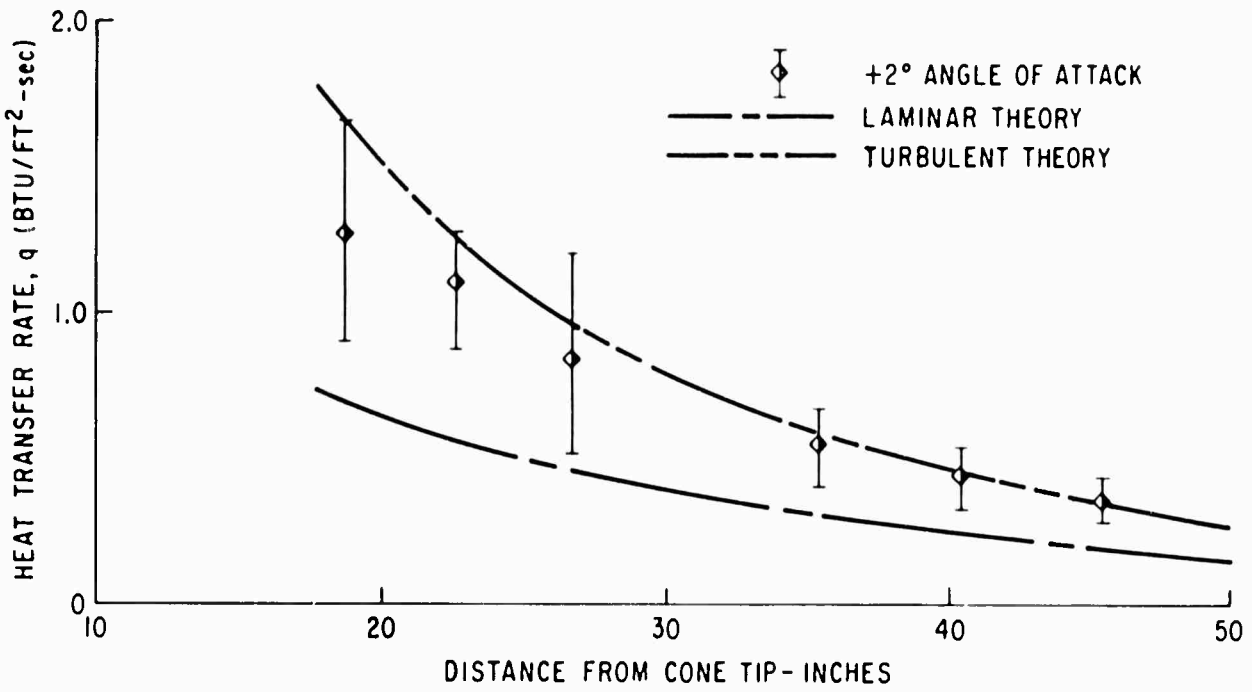

Fig. 23 Heat transfer distribution for smooth tip cone at +2° angle of attack: P_5 = 585 psia, T_5 = 1400°K.

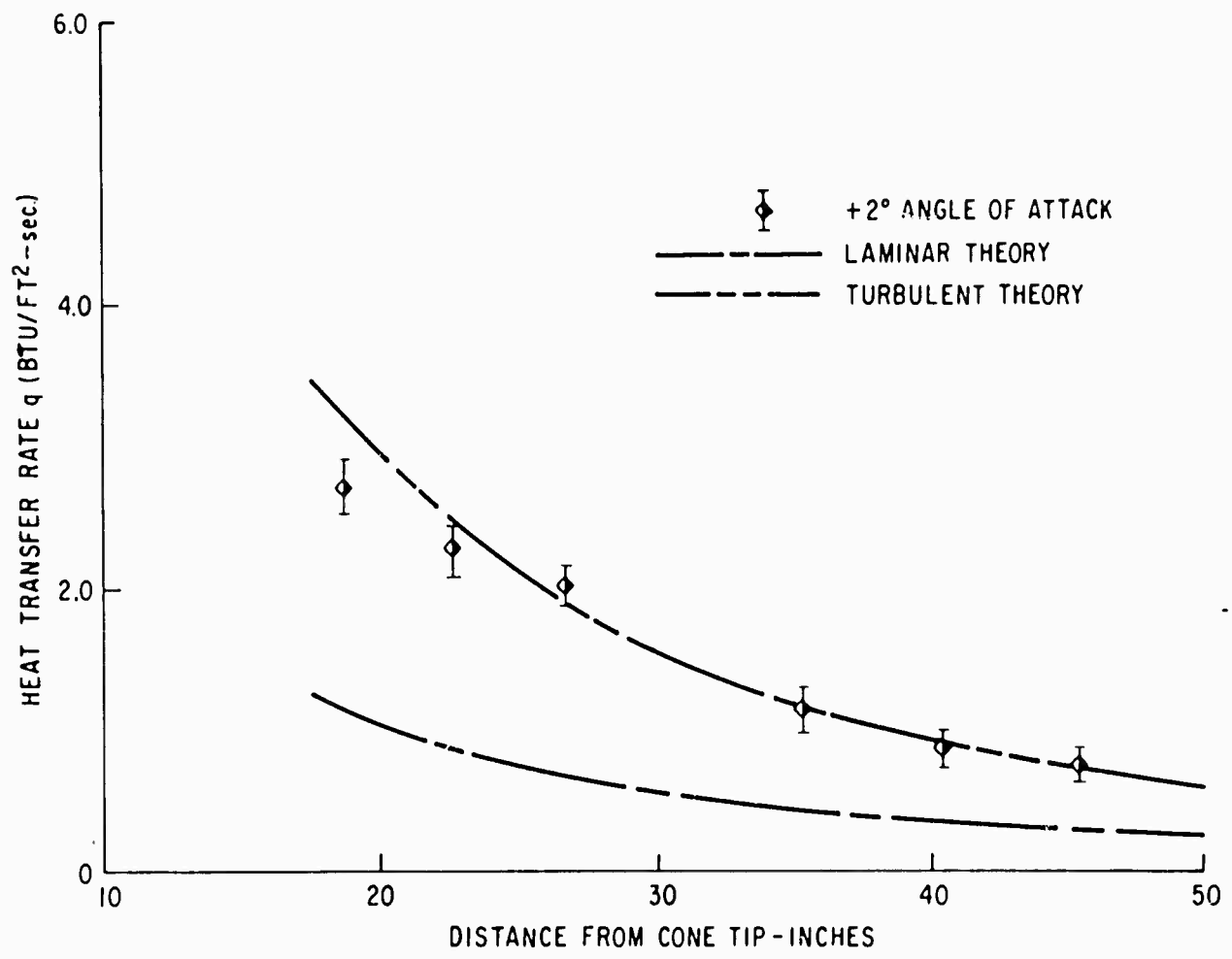

Fig. 24 Heat transfer distribution for smooth tip cone at +2° angle of attack: P_5 = 1300 psia, T_5 = 1400°K.

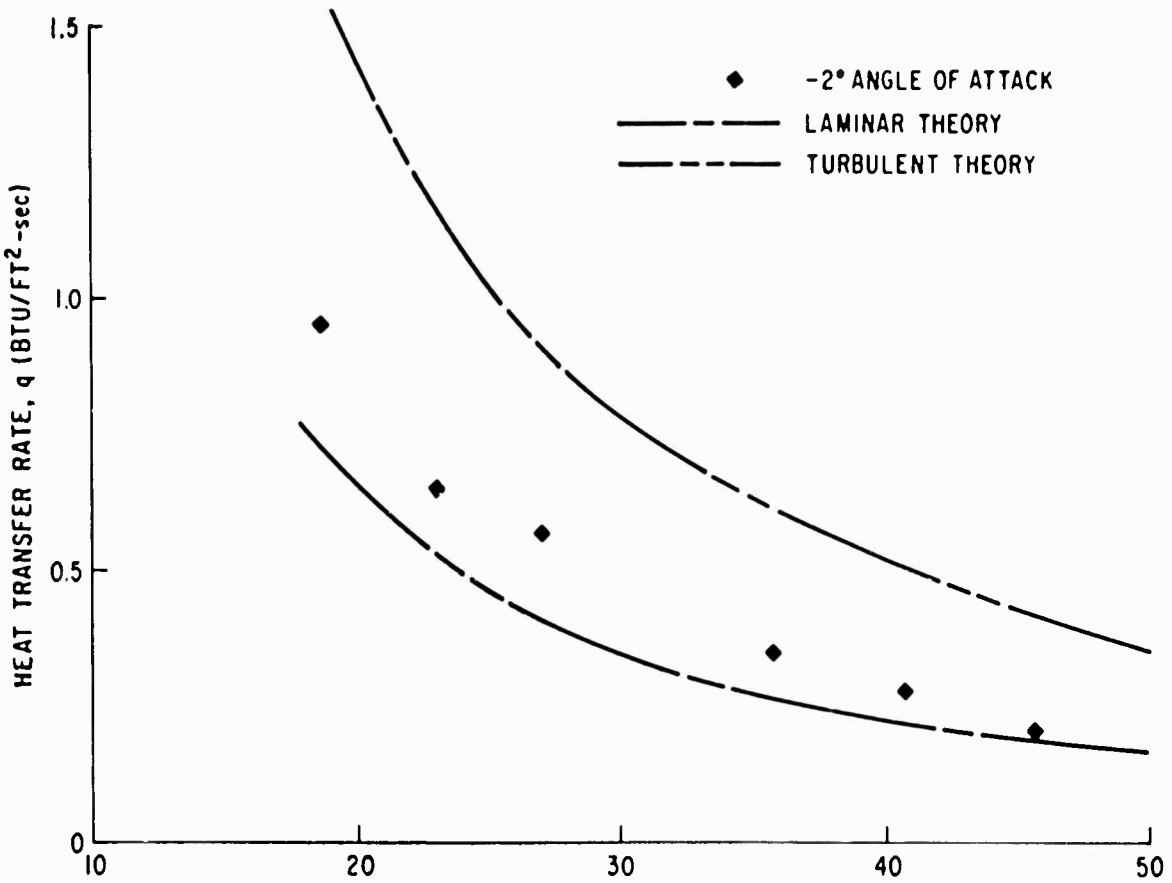

Fig. 25 Heat transfer distribution for smooth tip cone at -2° angle of attack: P_5 = 450 psia, T_5 = 1400°K.

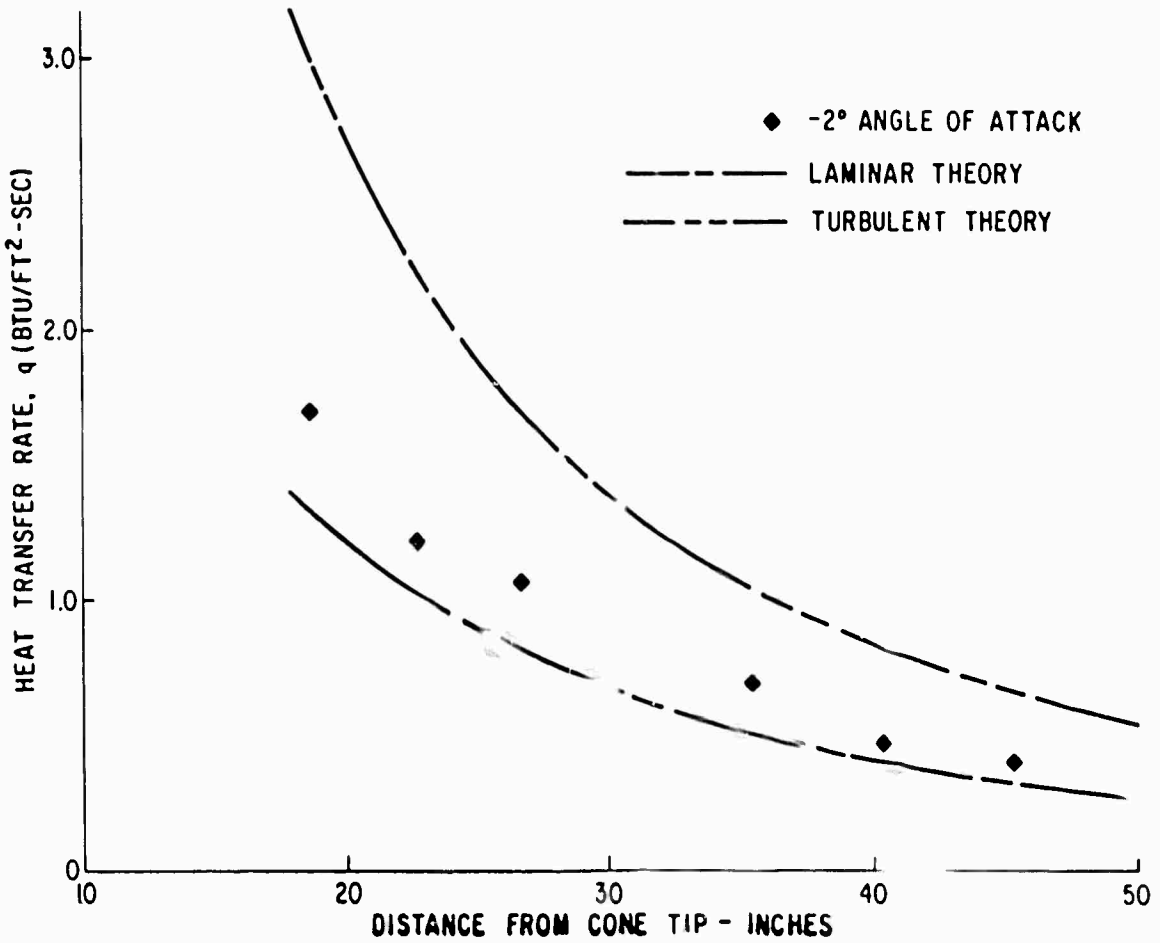

Fig. 26 Heat transfer distribution for smooth tip cone at -2° angle of attack: P_5 = 585 psia, T_5 = 1400°K.

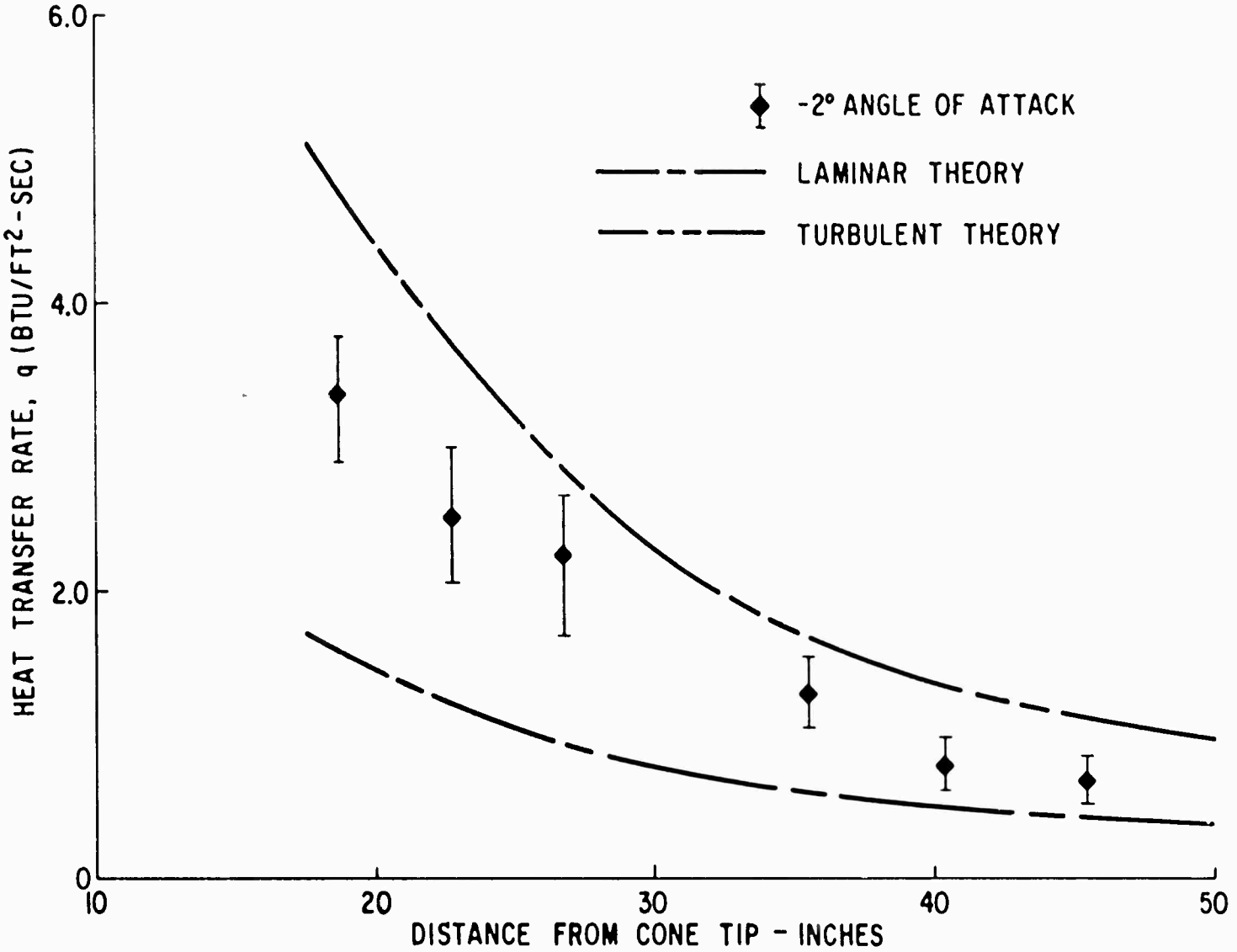

Fig. 27 Heat transfer distribution for smooth tip cone at -2° angle of attack: P_5 = 1300 psia, T_5 = 1400° K.

GENERAL ELECTRIC

Research Laboratory

SCHENECTADY, NEW YORK

TECHNICAL INFORMATION SERIES

Title Page

AUTHOR	SUBJECT CLASSIFICATION	NO.
Nagamatsu, H. T. Graber, B. C. Sheer, R. E., Jr.	hypersonics; fluid mechanics; gas dynamics	64-RL-(3829 C) DATE November 1964

TITLE: Roughness, Bluntness, and Angle of Attack Effects on Hypersonic Boundary Layer Transition

ABSTRACT: An investigation was conducted in a hypersonic shock tunnel to study the laminar boundary layer transition on a highly cooled 10° cone of 4-foot length over the Mach number range of 8.5 to 10.5 with a stagnation temperature of 1400°K. The effects on transition of tip surface roughness, tip bluntness, and ±2° angle of attack were investigated. With fast response thin film surface heat transfer gauges, it was possible to detect the passage of turbulent bursts that appeared at the beginning of transition. Boundary layer pitot tube surveys and schlieren photographs were obtained to verify the interpretation of the heat transfer data. It was found that the surface roughness greatly promoted transition in the proper Reynolds number range. The Reynolds number for the beginning and end of transition at the 8.5 Mach number location were 3.8×10^6 to 9.6×10^6 and 2.2×10^6 to 4.2×10^6 for the smooth sharp tip and rough sharp tip, respectively. The local skin friction data, determined from the pitot tube survey, agreed very well with the heat transfer data through Reynolds analogy. The tip bluntness data showed a strong delay in the beginning of transition for a cone base to tip diameter ratio of

(continued on back)

G.E. CLASS	REPRODUCIBLE COPY FILED AT	NO. PAGES
1	Research Information Section The Knolls Schenectady, New York	50
GOV. CLASS		

By cutting out this rectangle and folding on the center line, the above information can be fitted into a standard card file.

INFORMATION PREPARED FOR:

SECTION: Mechanical Investigations

DEPARTMENT: Chemistry Research